On the convergence of a low order Lagrange finite element approach for natural convection problems

C. Legrand, F. Luddens, I. Danaila

Université de Rouen Normandie
Laboratoire de Mathématiques Raphaël Salem, CNRS, UMR 6085
Avenue de l'Université, BP. 12
76801 Saint-Étienne-du-Rouvray, France

Abstract

The purpose of this article is to study the convergence of a low order finite element approximation for a natural convection problem. We prove that the discretization based on P_1 polynomials for every variable (velocity, pressure and temperature) is well-posed if used with a penalty term in the divergence equation, to compensate the loss of an inf-sup condition. With mild assumptions on the pressure regularity, we recover convergence for the Navier-Stokes-Boussinesq system, provided the penalty term is chosen in accordance with the mesh size. We express conditions to obtain optimal order of convergence. We illustrate theoretical convergence results with extensive examples. The computational cost that can be saved by this approach is also assessed.

1 Introduction

The finite element method was proved to be very effective for the numerical simulation of Phase Change Materials, described by Navier-Stokes equations supplemented with Boussinesq approximation for natural convection and an enthalpy model for the evolution of temperature. A common approach is to use a single domain method [1, 2] for the momentum equation. Projection schemes [3] or Newton based algorithms [1, 4] have been shown to give accurate results. Enthalpy models have been proven to be suitable for phase change, even with different thermophysical properties between the two phases, especially when combined with adaptive mesh refinement [5, 6].

The use of Taylor-Hood finite element for the velocity-pressure unknowns ensures convergence of the method [7]. The stability of the scheme is dictated by the inf-sup condition. Indeed, when this condition is uniformly satisfied at the discrete level, the well-posedness of the underlying problem is ensured. As a result, the pressure does not exhibit spurious modes. A large number of finite elements have been proven to satisfy the inf-sup condition, for instance the classical Taylor-Hood element. The lowest equal-order finite element P_1-P_1 pair does not satisfy this condition: the finite element space for the velocity is not rich enough to control the spurious pressure mode. Apparition of unphysical pressure oscillations has been highlighted in [8, section 5.2.5]. Several methods have been introduced to neutralize spurious modes. One of the commonly employed consist to enrich the velocity space in adding one degree of freedom per element, associated with the barycentre of the element. This new finite element, called P_{1b}, can be used for many different equations. In order to avoid the instability problem related to the choice of P_1 finite element for the velocity, several methods induce smaller discrete spaces for the pressure unknown and/or use an additional stabilization: projection stabilization [9, 10], the stabilization based on two local Gauss integrations [11, 12], symmetric pressure stabilization [13], and many others. This paper focuses on the stabilized finite element method based on minimal pressure stabilization procedures introduced by [14]. The aim of the study is to estimate the effect of changing the discrete problem to a penalized problem and get corresponding a priori error estimates.

There exists a vast literature on error estimations for Navier-Stokes equations. Error estimates for the Stokes problem in a bounded smooth domain with slip boundary condition have been established [15], using P_1-P_1 or P_{1b}-P_1 finite

element approximations and an additional penalty method on the boundary conditions. Estimation of the optimal order of convergence for the velocity and the pressure for the time-dependent Stokes equation with discrete inf-sup stable virtual space for $k \geq 2$ and non-divergence free is analysed in [16]. Several pressure stabilizations are studied in [17], with error analysis of time discretization schemes for corresponding Navier-Stokes equations.

For the natural convection problem with Boussinesq approximation, stability and convergence of the finite element method for the heat flow has been studied since [18]. Two-level finite-element have been employed in [19], the non-linearity beeing treated only at the coarse level. More recently, this problem has been analysed using a Backward Euler and a fully Crank-Nicolson scheme with a variational multi scale method and a stabilized term. Both schemes were proven to be unconditionally stable. Error bounds were derived for a finite element space discretization satisfying the inf-sup condition [12]. The stability of a finite element approximation scheme with inf-sup condition for phase change problems has been assessed in [20]. Assuming standard hypotheses on the discrete spaces, existence and stability of solutions of the Galerkin scheme associated to Navier-Stokes-Boussinesq equations can be obtained [21]. Corresponding Cea's estimate for smooth solutions can also be derived. The use of mini element P_{1b}-P_1 pair was analysed in [7]. A priori error estimates were derived for first and second order (in time) numerical schemes. Error bound using P_l-P_l pairs with ($l \geq 1$) have been established with different pressure stabilization, for example Local Projection Stabilization [10] or grad-div pressure stabilization [15].

This paper focuses on the approximation scheme introduced in [1]. A constant penalty term is added to the discretized mass conservation equation. From an algebraic point of view, this penalty term avoids the use of pivoting by eliminating a null block in the discretization matrix. It also ensures that the discrete pressure has zero average. We let this penalty term vary according to the mesh size, to recover convergence for the velocity and temperature unknowns, even if the inf-sup condition is not satisfied, e.g. for the P_1-P_1 pair. Using similar technique to [7], we give a priori estimates and numerical illustration to support the use of such elements.

The paper is organized as follows: in §2, we present the finite element approximation for the natural convection. The main result consists in Theorem 1 and is presented in §3, along with immediate corollaries illustrating the convergence of the numerical scheme. In §4, we introduce a modified projection operator onto the finite element space, and establish some approximation results. This operator allows us to prove Theorem 1 in §5. Finally, numerical results for the projection operator as well as the natural convection problem are reported in §6, in agreement with theoretical results.

2 Framework and discretization

2.1 Framework

Throughout the paper, Ω denotes a smooth bounded domain in $\mathbb{R}^2$. To use known regularity results, we assume that its boundary $\partial\Omega$ is of class $C^{1,1}$. We are interested in solving the natural convection problem modelled by the Navier-Stokes equations supplemented with the Boussinesq approximation.

Denoting by $\boldsymbol{u}$, p and θ the dimensionless velocity of the fluid, pressure and temperature respectively, the Navier-Stokes-Boussinesq system of equations reads:

$$\nabla \cdot \boldsymbol{u} = 0, \tag{1}$$

$$\frac{\partial \boldsymbol{u}}{\partial t} + (\boldsymbol{u}\nabla)\boldsymbol{u} + \nabla p - \frac{1}{Re}\nabla^2 \boldsymbol{u} - f_B(\theta)\,\boldsymbol{e}_y = \boldsymbol{F}, \tag{2}$$

$$\frac{\partial \theta}{\partial t} + \nabla \cdot (\theta \boldsymbol{u}) - \nabla \cdot \left(\frac{1}{RePr}\nabla\theta\right) = g. \tag{3}$$

f_B stands for the Boussinesq buoyancy force, assumed to be a linear function of the temperature:

$$f_B(\theta) = \frac{Ra}{PrRe^2}\theta. \tag{4}$$

We denote by Ra, Re and Pr the Rayleigh, Reynolds and Prandtl numbers respectively. Finally, $\boldsymbol{F}$ and g denote external force and heat source.

The system (1)-(2)-(3) is supplemented with Dirichlet boundary conditions on $\boldsymbol{u}$ and θ.

2.2 Weak formulation

To use finite element approximations, a weak formulation of the previous system is needed. We introduce classical Hilbert spaces :

$$X = H_0^1(\Omega), \quad Q = \left\{ q \in L^2(\Omega) \mid \int_\Omega q = 0 \right\}, \quad \boldsymbol{X} = X \times X, \tag{5}$$

and define the following bilinear and trilinear forms: for $\boldsymbol{u}, \boldsymbol{v}, \boldsymbol{w} \in \boldsymbol{X}$, $p \in Q$ and $\theta, \psi \in X$,

$$\begin{aligned}
a(\boldsymbol{u}, \boldsymbol{v}) &= (\nabla \boldsymbol{u}, \nabla \boldsymbol{v}), & (6)\\
\bar{a}(\theta, \phi) &= (\nabla \theta, \nabla \phi), & (7)\\
b(\boldsymbol{u}, p) &= -(\nabla \cdot \boldsymbol{u}, p), & (8)\\
c(\boldsymbol{u}, \boldsymbol{v}, \boldsymbol{w}) &= \frac{1}{2}(\boldsymbol{u}\nabla \boldsymbol{v}, \boldsymbol{w}) - \frac{1}{2}(\boldsymbol{u}\nabla \boldsymbol{w}, \boldsymbol{v}), & (9)\\
\bar{c}(\boldsymbol{u}, \theta, \psi) &= \frac{1}{2}(\boldsymbol{u}\nabla \theta, \boldsymbol{\psi}) - \frac{1}{2}(\boldsymbol{u}\nabla \psi, \theta), & (10)
\end{aligned}$$

where $(u, v) = \int_\Omega u \cdot v$ denotes the scalar product in $L^2(\Omega)$. If $\boldsymbol{u} \in \boldsymbol{X}$ is such that $\nabla \cdot \boldsymbol{u} = 0$, operators (9)-(10) are equivalent to

$$c(\boldsymbol{u}, \boldsymbol{v}, \boldsymbol{w}) = (\boldsymbol{u}\nabla \boldsymbol{v}, \boldsymbol{w}) = \int_\Omega (\boldsymbol{u}\nabla \boldsymbol{v}) \cdot \boldsymbol{w}, \tag{11}$$

$$\bar{c}(\boldsymbol{u}, \theta, \psi) = (\boldsymbol{u}\nabla \theta, \psi) = \int_\Omega (\boldsymbol{u}\nabla \theta)\, \psi. \tag{12}$$

If $(\boldsymbol{u}, p, \theta)$ is a solution to Eqns. (1)-(2)-(3) and $(\boldsymbol{v}, q, \psi) \in \boldsymbol{X} \times L^2 \times X$, we obtain by integration by parts the following weak formulation:

$$\begin{aligned}
b(\boldsymbol{u}, q) &= 0, & (13)\\
\left(\frac{\partial \boldsymbol{u}}{\partial t}, \boldsymbol{v}\right) + \frac{1}{Re} a(\boldsymbol{u}, \boldsymbol{v}) + c(\boldsymbol{u}, \boldsymbol{u}, \boldsymbol{v}) + b(\boldsymbol{v}, p) - (f_B(\theta)\boldsymbol{e}_y, \boldsymbol{v}) &= (\boldsymbol{F}, \boldsymbol{v}), & (14)\\
\left(\frac{\partial \theta}{\partial t}, \psi\right) + \frac{1}{RePr} \bar{a}(\theta, \psi) + \bar{c}(\boldsymbol{u}, \theta, \psi) &= (g, \psi). & (15)
\end{aligned}$$

2.3 Properties of bilinear and trilinear forms

From definitions (6)-(10), the following classical coercivity and continuity estimates hold: there exist some positive constants $\alpha, \bar{\alpha}, A, \bar{A}$ such that, $\forall \boldsymbol{u}, \boldsymbol{v} \in \boldsymbol{X}$, $\forall p \in Q$ and $\forall \theta, \phi \in X$,

$$\begin{aligned}
|a(\boldsymbol{u}, \boldsymbol{v})| &\leq A \|\boldsymbol{u}\|_{H^1} \|\boldsymbol{v}\|_{H^1}, & (16)\\
|a(\boldsymbol{v}, \boldsymbol{v})| &\geq \alpha \|\boldsymbol{v}\|_{H^1}, & (17)\\
|\bar{a}(\theta, \phi)| &\leq \bar{A} \|\theta\|_{H^1} \|\phi\|_{H^1}, & (18)\\
|\bar{a}(\theta, \theta)| &\geq \bar{\alpha} \|\theta\|_{H^1}, & (19)\\
|b(\boldsymbol{u}, p)| &\leq \|\boldsymbol{u}\|_{H^1} \|p\|_{L^2}. & (20)
\end{aligned}$$

We also use the continuity of trilinear forms c and $\bar{c}$: there exist positive constants C and $\bar{C}$ such that, $\forall \boldsymbol{u}, \boldsymbol{v}, \boldsymbol{w} \in \boldsymbol{X}$ and $\forall \theta, \psi \in X$,

$$c(\boldsymbol{u}, \boldsymbol{v}, \boldsymbol{w}) \leq C \|\nabla \boldsymbol{u}\|_{L^2} \|\nabla \boldsymbol{v}\|_{L^2} \|\boldsymbol{w}\|_{L^2}^{\frac{1}{2}} \|\nabla \boldsymbol{w}\|_{L^2}^{\frac{1}{2}}, \tag{21}$$

$$\bar{c}(\boldsymbol{u}, \theta, \psi) \leq \bar{C} \|\nabla \boldsymbol{u}\|_{L^2} \|\nabla \theta\|_{L^2} \|\psi\|_{L^2}^{\frac{1}{2}} \|\nabla \psi\|_{L^2}^{\frac{1}{2}}. \tag{22}$$

Owing to skew-symmetry properties, $\boldsymbol{v}$ and $\boldsymbol{w}$ can be swapped in the right hand side of (21), and similarly θ and ψ in the right hand side of (22). In order to get the best possible convergence rate for the natural convection problem, we rely on the continuity result of the following Proposition 1 that holds in the two-dimensional case.

Proposition 1. *For any $\sigma > 0$, there exists a positive constant C depending only on Ω and σ such that*

$$\forall \boldsymbol{u}, \boldsymbol{v}, \boldsymbol{w}, \in \boldsymbol{X}, \qquad |c(\boldsymbol{u}, \boldsymbol{v}, \boldsymbol{w})| \leq C \|\boldsymbol{u}\|_{H^\sigma} \|\boldsymbol{v}\|_{H^1} \|\boldsymbol{w}\|_{H^1}, \tag{23}$$

$$\forall \boldsymbol{u}, \boldsymbol{v}, \boldsymbol{w}, \in \boldsymbol{X}, \qquad |c(\boldsymbol{u}, \boldsymbol{v}, \boldsymbol{w})| \leq C \|\boldsymbol{v}\|_{H^\sigma} \|\boldsymbol{u}\|_{H^1} \|\boldsymbol{w}\|_{H^1}. \tag{24}$$

Proof. We start with $0 < \sigma < 1$. Note that if (23) holds for $0 < \sigma < 1$, then it holds for any $\sigma' > \sigma$.

From Cauchy-Schwarz and Holder inequalities, we have

$$\left| \int_\Omega \boldsymbol{u} \nabla \boldsymbol{v} \boldsymbol{w} \right| \leq \|\nabla \boldsymbol{v}\|_{L^2} \|\boldsymbol{u}\boldsymbol{w}\|_{L^2} \leq \|\nabla \boldsymbol{v}\|_{L^2} \|\boldsymbol{u}\|_{L^q} \|\boldsymbol{w}\|_{L^{q^*}},$$

where $q > 2$ is such that $\sigma = 1 - \frac{2}{q}$ and q^* is such that $\frac{1}{q} + \frac{1}{q^*} = \frac{1}{2}$. The injections $L^q \subset H^\sigma$ and $L^{q^*} \subset H^1$ are continuous (see [22]), so that

$$\left| \int_\Omega \boldsymbol{u} \nabla \boldsymbol{v} \boldsymbol{w} \right| \leq C \|\nabla \boldsymbol{v}\|_{L^2} \|\boldsymbol{u}\|_{H^\sigma} \|\boldsymbol{w}\|_{H^1} \leq C \|\boldsymbol{u}\|_{H^\sigma} \|\boldsymbol{v}\|_{H^1} \|\boldsymbol{w}\|_{H^1}.$$

From this inequality, we also obtain

$$\left| \int_\Omega \boldsymbol{u} \nabla \boldsymbol{w} \boldsymbol{v} \right| \leq C \|\boldsymbol{u}\|_{H^\sigma} \|\boldsymbol{v}\|_{H^1} \|\boldsymbol{w}\|_{H^1}.$$

Gathering the two inequalities, together with the definition of c yields the desired result (23).

In order to prove (24), we use the fact that

$$c(\boldsymbol{u}, \boldsymbol{v}, \boldsymbol{w}) = -\int_\Omega \boldsymbol{u} \nabla \boldsymbol{w} \boldsymbol{v} - \frac{1}{2} \int_\Omega (\nabla \cdot \boldsymbol{u}) \boldsymbol{v} \boldsymbol{w}.$$

We proceed as before : the first term is treated using $\|\boldsymbol{u}\boldsymbol{v}\|_{L^2}$, and the second one with $\|\boldsymbol{w}\boldsymbol{v}\|_{L^2}$.

□

Finally, we recall that $\boldsymbol{X} \times Q$ satisfies the inf-sup condition (also called LBB condition, e.g. [23]): there exists $\beta > 0$ only depending on Ω such that, for all $p \in Q$,

$$\beta \|p\|_{L^2} \leq \sup_{\boldsymbol{u} \in \boldsymbol{X} \setminus \{0\}} \frac{b(\boldsymbol{u}, p)}{\|\boldsymbol{u}\|_{H^1}}. \tag{25}$$

2.4 Finite element approximation

Let us introduce a family of uniform and regular meshes $\mathcal{T}_h$, indexed by h (typically the size of a triangle). Given an integer ℓ, and an element $K \in \mathcal{T}_h$, we denote by $P_\ell(K)$ the space of polynomials of degree less than, or equal to ℓ, defined on K. We introduce the following finite element spaces

$$X_h := \{v_h \in C(\Omega)^d; v_h|_K \in P_{p_u}(K)^d, \quad \forall K \in \mathcal{T}_h\} \tag{26}$$

$$Q_h := \{q_h \in C(\Omega)^d; q_h|_K \in P_{p_p}(K)^d, \quad \forall K \in \mathcal{T}_h\} \tag{27}$$

$$W_h := \{w_h \in C(\Omega)^d; w_h|_K \in P_{p_\theta}(K)^d, \quad \forall K \in \mathcal{T}_h\} \tag{28}$$

where $p_u \geq 1$, $p_p \geq 1$ and $p_\theta \geq 1$. In the applications, we want to use $p_u = p_p = p_\theta = 1$.

We are interested in the approximation of the natural convection problem for $t \in [0; t_f]$ where t_f is a given final time. Let us choose N_f a number of time steps, and define $\delta t = \frac{t_f}{N_f}$. We denote by $t_n = n\delta t$ for any integer n and $(\boldsymbol{u}_h^n, p_h^n, \theta_h^n) \in X_h \times Q_h \times W_h$ our approximation of $(\boldsymbol{u}^n, p^n, \theta^n)$, where $\boldsymbol{u}^n$ stands for $\boldsymbol{u}(t_n)$ (the same for p^n, θ^n). Introducing the notations

$$\delta_t \boldsymbol{u}_h^n = \frac{\boldsymbol{u}_h^n - \boldsymbol{u}_h^{n-1}}{\delta t}, \quad \delta_t \theta_h^n = \frac{\theta_h^n - \theta_h^{n-1}}{\delta t},$$

the discretized system corresponding to (13)-(15) is:

Find $(\boldsymbol{u}_h^{n+1}, p_h^{n+1}, \theta_h^{n+1})$ such that, for any $(\boldsymbol{v}_h, q_h, \psi_h) \in X_h \times Q_h \times W_h$,

$$b(\boldsymbol{u}_h^{n+1}, q_h) - \gamma_h(p_h^{n+1}, q_h) = 0, \tag{29}$$

$$\begin{aligned}\left(\delta_t \boldsymbol{u}_h^{n+1}, \boldsymbol{v}_h\right) + \frac{1}{Re} a(\boldsymbol{u}_h^{n+1}, \boldsymbol{v}_h) + c(\boldsymbol{u}_h^{n+1}, \boldsymbol{u}_h^{n+1}, \boldsymbol{v}_h) \\ + b(\boldsymbol{v}_h, p_h^{n+1}) - \left(f_B(\theta_h^{n+1})\boldsymbol{e}_y, \boldsymbol{v}_h\right) = \left(\boldsymbol{F}^{n+1}, \boldsymbol{v}_h\right),\end{aligned} \tag{30}$$

$$\left(\delta_t \theta_h^{n+1}, \psi_h\right) + \frac{1}{RePr} \bar{a}(\theta_h^{n+1}, \psi_h) + \bar{c}(\boldsymbol{u}_h^{n+1}, \theta_h^{n+1}, \psi_h) = \left(g^{n+1}, \psi_h\right). \tag{31}$$

The resulting system is a non linear problem solved using a Newton algorithm, as in [1]. γ_h is a positive constant that might depend on the mesh size. This penalty parameter is the key player in our analysis, and deserve some remarks:

- it is well-known that, using Taylor-Hood element for the velocity-pressure for example allows one to use $\gamma_h = 0$. However, from a computational point of view, this leads to a invertible matrix with a zero diagonal block. Hence, it requires some pivoting. Letting $\gamma_h > 0$ removes the necessity of using pivots.
- since Q_h is not a subspace of Q (there is no constraint on the mean value of an element of Q_h), taking $\gamma_h > 0$ together with the boundary conditions on $\boldsymbol{u}_h$ and the Stokes formula ensures that the pressure has zero mean value. In this respect, this term can be viewed as a *penalty* term.
- even if the couple $X_h \times Q_h$ does not satisfy an inf-sup condition, taking $\gamma_h > 0$ will provide the well-posedness of the linearised system, allowing the use of the Lax-Milgram lemma. In this respect, it can also be viewed as a *stabilization* term. See also details in [24, Rem. 4.3, p. 67].
- it is clear that using a constant value for γ_h cannot lead to convergence when h goes to zero. We will show however that, with a suitable choice of γ_h, we can obtain convergence for our problem.

Let us conclude this section with the introduction of suitable projection operators. We assume that there exists a family of operators $\mathcal{C}_h : L^2(\Omega) \to Q_h$ that satisfies the following properties: there exists C independent of h such that, for any $0 \leqslant s < \frac{3}{2}$, $s \leqslant r \leqslant 1 + p_p$ and $q \in H^r(\Omega)$, the following inequality holds:

$$\|q - \mathcal{C}_h q\|_{H^s} \leq C h^{r-s} \|q\|_{H^r}. \tag{32}$$

As projection operators, one might think of the Clément interpolant, or the Scott-Zhang interpolant [25]. Abusing the notations, we also denote by $\mathcal{C}_h$ the H^1 projections from $\boldsymbol{X}$ to X_h and from X to W_h. For these operators, (32) is also satisfied since it can be inferred from their definitions

$$a(\mathcal{C}_h \boldsymbol{u}, \boldsymbol{v}_h) = a(\boldsymbol{u}, \boldsymbol{v}_h) \qquad \forall \boldsymbol{u} \in \boldsymbol{X}, \boldsymbol{v}_h \in X_h, \tag{33}$$

$$\bar{a}(\mathcal{C}_h \theta, \psi_h) = \bar{a}(\theta, \psi_h) \qquad \forall \theta \in X, \psi_h \in W_h. \tag{34}$$

3 Main convergence result

3.1 Notations and assumptions

Let $0 < \sigma < 1$ (close to 0) and define $\tilde{\theta}_h^n = \mathcal{C}_h \theta^n$. We define $(\tilde{\boldsymbol{u}}_h^n, \tilde{p}_h^n) = \mathbb{P}_{\gamma_h,0}^{X_h,Q_h}(\boldsymbol{u}^n, p^n)$, that is: for any $\boldsymbol{v}_h \in X_h$ and any $q_h \in Q_h$,

$$\frac{1}{Re} a(\tilde{\boldsymbol{u}}_h^n, \boldsymbol{v}_h) + b(\boldsymbol{v}_h, \tilde{p}_h^n) - b(\tilde{\boldsymbol{u}}_h^n, q_h) + \gamma_h(\tilde{p}_h^n, q_h) = \frac{1}{Re} a(\boldsymbol{u}^n, \boldsymbol{v}_h) + b(\boldsymbol{v}_h, p^n) - b(\boldsymbol{u}^n, q_h).$$

The approximations properties of this operator are detailed in Section 4. The errors are decomposed as:

$$\begin{aligned}
\boldsymbol{e}_u^n &= \boldsymbol{u}^n - \boldsymbol{u}_h^n = (\boldsymbol{u}^n - \tilde{\boldsymbol{u}}_h^n) - (\boldsymbol{u}_h^n - \tilde{\boldsymbol{u}}_h^n) = \eta_u^n - \varphi_u^n, \\
e_p^n &= p^n - p_h^n = (p^n - \tilde{p}_h^n) - (p_h^n - \tilde{p}_h^n) = \eta_p^n - \varphi_p^n, \\
e_\theta^n &= \theta^n - \theta_h^n = \left(\theta^n - \tilde{\theta}_h^n\right) - \left(\theta_h^n - \tilde{\theta}_h^n\right) = \eta_\theta^n - \varphi_\theta^n.
\end{aligned}$$

We also define R_u^n and R_θ^n as :

$$R_u^n = \partial_t \boldsymbol{u}^n - \delta_t \boldsymbol{u}^n, \quad R_\theta^n = \partial_t \theta^n - \delta_t \theta^n.$$

We can use $(\boldsymbol{v}_h, q_h, \psi_h) \in X_h \times Q_h \times W_h$, as a test function in the weak formulation (13)-(14)-(15) at time t_{n+1} so that:

$$b(\boldsymbol{u}^{n+1}, q_h) = 0, \tag{35}$$

$$\begin{aligned}
\left(\delta_t \boldsymbol{u}^{n+1}, \boldsymbol{v}_h\right) + \frac{1}{Re} a(\boldsymbol{u}^{n+1}, \boldsymbol{v}_h) + c(\boldsymbol{u}^{n+1}, \boldsymbol{u}^{n+1}, \boldsymbol{v}_h) & \\
+ b(\boldsymbol{v}_h, p^{n+1}) - \left(f_B(\theta^{n+1}) \boldsymbol{e}_y, \boldsymbol{v}_h\right) &= \left(\boldsymbol{F}^{n+1}, \boldsymbol{v}_h\right) - \left(R_u^{n+1}, \boldsymbol{v}_h\right), \qquad (36) \\
\left(\delta_t \theta^{n+1}, \psi_h\right) + \frac{1}{RePr} \bar{a}(\theta^{n+1}, \psi_h) + \bar{c}(\boldsymbol{u}^{n+1}, \theta^{n+1}, \psi_h) &= \left(g^{n+1}, \psi_h\right) - \left(R_\theta^{n+1}, \psi_h\right). \qquad (37)
\end{aligned}$$

In this article, we focus on solutions that exhibit mild regularity properties. This is expressed by the following assumptions.

Assumption 1. *$\boldsymbol{u}$ and θ are bounded in H^1 and p is bounded in L^2, and we introduce $\mathcal{N} > 0$ such that*

$$\forall t \in [0; t_f], \qquad \|\boldsymbol{u}(t)\|_{H^1} + \|p(t)\|_{L^2} + \|\theta(t)\|_{H^1} \leq \mathcal{N}. \tag{38}$$

Assumption 2. *There exists $0 \leq s_\theta \leq p_\theta$ such that $\boldsymbol{u} \in L^\infty(0, t_f; H^2)$, $\partial_t \boldsymbol{u} \in L^\infty(0, t_f; H^2)$, $\partial_{tt} \boldsymbol{u} \in L^\infty(0, t_f; L^2)$, $p \in L^\infty(0, t_f; H^1)$, $\partial_t p \in L^\infty(0, t_f; H^1)$, $\theta \in L^\infty(0, t_f; H^{1+s_\theta})$, $\partial_t \theta \in L^\infty(0, t_f; H^{s_\theta})$, $\partial_{tt} \theta \in L^\infty(0, t_f; L^2)$. We then introduce*

$$\begin{aligned}
M_2(\boldsymbol{u}, p, \theta) := \|\partial_{tt} \boldsymbol{u}\|^2_{L^\infty(L^2)} + \|\partial_{tt} \theta\|^2_{L^\infty(L^2)} + \|\theta\|^2_{L^\infty(H^{1+s_\theta})} & \qquad (39) \\
+ \|\partial_t \theta\|^2_{L^\infty(H^{s_\theta})} + \|\boldsymbol{u}\|^2_{L^\infty(H^2)} + \|p\|^2_{L^\infty(H^1)} & \qquad (40) \\
+ \|p\|^2_{L^\infty(L^2)} + \|\boldsymbol{u}\|^4_{L^\infty(H^2)} + \|p\|^4_{L^\infty(H^1)} & \qquad (41) \\
+ \|p\|^4_{L^\infty(L^2)} + \|\partial_t \boldsymbol{u}\|^2_{L^\infty(H^2)} + \|\partial_t p\|^2_{L^\infty(H^1)} + \|\partial_t p\|^2_{L^\infty(L^2)} & \qquad (42)
\end{aligned}$$

Note that Assumption 1 is redundant with Assumption 2, but we keep it in order to separate terms that are bounded by $\mathcal{N}$ from those bounded by M_2. Throughout the paper, we will denote by C a positive constant that is independent of h and M_2. Unless stated otherwise, C might depend on $\mathcal{N}$, Ω, σ and/or the dimensionless parameters Re, Pr and Ra. Its value may change at every line.

Theorem 1. *Let $(\boldsymbol{u}, p, \theta)$ be the solution of (1)-(2)-(3) such that Assumptions 1 and 2 hold. Let $0 < \sigma < 1$ be a small real number. Then the following error estimates holds for any $n \leqslant N_f$:*

$$\begin{aligned}
&\|\varphi_u^n\|_0^2 + \|\varphi_\theta^n\|_0^2 \leq C\Big(\delta t^2 \|\partial_{tt}\boldsymbol{u}\|^2_{L^\infty(L^2)} + \delta t^2 \|\partial_{tt}\theta\|^2_{L^\infty(L^2)} + h^{2s_\theta}\|\theta\|^2_{L^\infty(H^{1+s_\theta})} \\
&+ h^{2s_\theta}\|\partial_t\theta\|^2_{L^\infty(H^{s_\theta})} + \frac{h^{4-2\sigma}}{\gamma_h^{2-\sigma}}\|\boldsymbol{u}\|^2_{L^\infty(H^2)} + \frac{h^{4-\sigma}}{\gamma_h^{2-\sigma}}\|p\|^2_{L^\infty(H^1)} \\
&+ \gamma_h^2\|p\|^2_{L^\infty(L^2)} + \frac{h^4}{\gamma_h^2}\|\boldsymbol{u}\|^4_{L^\infty(H^2)} + \frac{h^4}{\gamma_h^2}\|p\|^4_{L^\infty(H^1)} \\
&+ \gamma_h^4\|p\|^4_{L^\infty(L^2)} + \frac{h^4}{\gamma_h^2}\|\partial_t\boldsymbol{u}\|^2_{L^\infty(H^2)} + \frac{h^4}{\gamma_h^2}\|\partial_t p\|^2_{L^\infty(H^1)} + \gamma_h^2\|\partial_t p\|^2_{L^\infty(L^2)}\Big)
\end{aligned} \tag{43}$$

The proof of this theorem is postponed to Section 5. To get a convergence result, we need the following corollary to this result.

Corollary 1. *Under the assumptions of Theorem 1, the following error estimate holds, for $h^2 < \gamma_h < 1$:*

$$\|\boldsymbol{e}_u^n\|_0^2 + \|e_\theta^n\|_0^2 \leq C\left(\delta t^2 + h^{2s_\theta} + \frac{h^{4-2\sigma}}{\gamma_h^{2-\sigma}} + \gamma_h^2\right) M_2(\boldsymbol{u}, p, \theta). \tag{44}$$

Proof. Using the triangular inequality, we obtain

$$\|\boldsymbol{e}_u^n\|_0^2 + \|e_\theta^n\|_0^2 \leq 2\|\varphi_u^n\|_0^2 + 2\|\varphi_\theta^n\|_0^2 + 2\|\eta_u^n\|_0^2 + 2\|\eta_\theta^n\|_0^2.$$

The first two terms correspond to the left hand side of (43), so that

$$\|\varphi_u^n\|_0^2 + \|\varphi_\theta^n\|_0^2 \leq \left(\delta t^2 + h^{2s_\theta} + \frac{h^{4-2\sigma}}{\gamma_h^{2-\sigma}} + \gamma_h^2\right) M_2(\boldsymbol{u}, p, \theta).$$

For the last two terms, we use the properties of $\mathcal{C}_h$ and $\tilde{\boldsymbol{u}}_h$, see Eqns. (32) and (71)

$$\begin{aligned}
\|\eta_u^n\|_0^2 = \|\boldsymbol{u}^n - \tilde{\boldsymbol{u}}_h^n\|_0^2 &\leq C\left(\frac{h^4}{\gamma_h^2}\|\boldsymbol{u}^n\|^2_{H^2} + \frac{h^4}{\gamma_h}\|p^n\|^2_{H^1} + \gamma_h^2\|p^n\|^2_{L^2}\right) \\
&\leq C\left(\frac{h^4}{\gamma_h^2} + \frac{h^4}{\gamma_h} + \gamma_h^2\right) M_2(\boldsymbol{u}, p, \theta), \\
\|\eta_\theta^n\|_0^2 = \|\theta^n - \mathcal{C}_h\theta^n\|_0^2 &\leq Ch^{2+2s_\theta}\|\theta^n\|^2_{H^{1+s_\theta}} \leq Ch^{2+2p_\theta} M_2(\boldsymbol{u}, p, \theta).
\end{aligned}$$

Owing to the assumptions on γ_h, the latter right hand sides are bounded by the right hand side of (44). □

Remark 1. *The convergence rate is not limited by s_θ, therefore we can set $s_\theta = 1$ (e.g. $p_\theta = 1$ means that we also use P_1 elements for θ). Then the estimate becomes*

$$\|\boldsymbol{e}_u^n\|_0^2 + \|e_\theta^n\|_0^2 \leq C\left(\delta t^2 + h^2 + \frac{h^{4-2\sigma}}{\gamma_h^{2-\sigma}} + \gamma_h^2\right) M_2(\boldsymbol{u}, p, \theta).$$

If we choose $\gamma_h = h$, then we obtain

$$\|\boldsymbol{e}_u^n\|_0^2 + \|e_\theta^n\|_0^2 \leq C\left(\delta t^2 + h^{2-\sigma}\right) M_2(\boldsymbol{u}, p, \theta)$$

and we get an almost first order accuracy in h, supported by our numerical results, see Section 6.

Remark 2. *In Theorem 1 and its corollary, the constant C depends on σ and goes to infinity as $\sigma \to 0$. Hence, we do not recover the maximal order of convergence, but we can be as close as desired.*

4 Modified Stokes projection

It is possible to establish a convergence result, similar to Theorem 1, by using $\mathcal{C}_h\boldsymbol{u}$ and $\mathcal{C}_h p$ instead of $\tilde{\boldsymbol{u}}_h$ and $\tilde{p}_h$. However, this leads to a predicted convergence order of $1/2$ in space, which is clearly not optimal. The purpose of this section is to design a modified Stokes projection that will help to improve the convergence rate. We call it *modified Stokes projection* since, strictly speaking, it is not a projection.

4.1 Definition of a family of operators

Definition 1. *For any $0 \leq \lambda < 1$, we define the bilinear form a_λ on $\boldsymbol{X} \times L^2$ by*

$$a_\lambda\big((\boldsymbol{u},p),(\boldsymbol{v},q)\big) := \frac{1}{Re}a(\boldsymbol{u},\boldsymbol{v}) + b(\boldsymbol{v},p) - b(\boldsymbol{u},q) + \lambda(p,q).$$

We introduce a norm adapted to this bilinear form, viz.

$$\|\boldsymbol{u},p\|_\lambda := \frac{1}{\sqrt{Re}}\|\boldsymbol{u}\|_{H^1} + \sqrt{\lambda}\|p\|_{L^2}.$$

In the following, we will always assume that $0 < \lambda < 1$ and that $Re > 1$.

Proposition 2. *a_λ is coercive and continuous with respect to the norm $\|\cdot\|_\lambda$. More precisely, there exist C, C' independent of λ and Re such that, for any $(\boldsymbol{u},p) \in \boldsymbol{X} \times L^2$ and $(\boldsymbol{v},q) \in \boldsymbol{X} \times L^2$,*

$$C'\|\boldsymbol{u},p\|_\lambda^2 \leq a_\lambda\big((\boldsymbol{u},p),(\boldsymbol{u},p)\big), \tag{45}$$

$$\big|a_\lambda\big((\boldsymbol{u},p),(\boldsymbol{v},q)\big)\big| \leq \frac{C\sqrt{Re}}{\sqrt{\lambda}}\|\boldsymbol{u},p\|_\lambda\|\boldsymbol{v},q\|_\lambda. \tag{46}$$

The coercivity of a_λ directly derives from that of the bilinear form a, while the continuity is obtained from the continuity of a and b and Cauchy-Schwarz inequalities. Using this bilinear form, we define a family of operators in the following way:

Definition 2. *Let $\mathcal{X}$ be a closed subset of $\boldsymbol{X}$ and $\mathcal{Q}$ be a closed subset of L^2. For any $0 < \lambda < 1$ and $0 \leq \gamma < 1$, we define the operator $\mathbb{P}_{\lambda,\gamma}^{\mathcal{X},\mathcal{Q}} : \boldsymbol{X} \times L^2 \to \mathcal{X} \times \mathcal{Q}$ in a weak form. For any $(\boldsymbol{u},p) \in \boldsymbol{X} \times L^2$, $\mathbb{P}_{\lambda,\gamma}^{\mathcal{X},\mathcal{Q}}(\boldsymbol{u},p) = (\tilde{\boldsymbol{u}},\tilde{p}) \in \mathcal{X} \times \mathcal{Q}$ is such that:*

$$\forall(\boldsymbol{v},q) \in \mathcal{X} \times \mathcal{Q}, \qquad a_\lambda\big((\tilde{\boldsymbol{u}},\tilde{p}),(\boldsymbol{v},q)\big) = a_\gamma\big((\boldsymbol{u},p),(\boldsymbol{v},q)\big). \tag{47}$$

Owing to the coercivity and continuity of a_λ, the operators $\mathbb{P}_{\lambda,\gamma}^{\mathcal{X},\mathcal{Q}}$ are well-defined. We want to use the operator $\mathbb{P}_{\gamma_h,0}^{X_h,Q_h}$ to establish convergence results for the natural convection problem. Note that, owing to (47), for $(\boldsymbol{u},p) \in \boldsymbol{X} \times L^2$, if we define $(\boldsymbol{u}_h,p_h) = \mathbb{P}_{\gamma_h,0}^{X_h,Q_h}(\boldsymbol{u},p)$ and $(\tilde{\boldsymbol{u}},\tilde{p}) = \mathbb{P}_{\gamma_h,0}^{\boldsymbol{X},L^2}(\boldsymbol{u},p)$, then we have

$$(\boldsymbol{u}_h,p_h) = \mathbb{P}_{\gamma_h,\gamma_h}^{X_h,Q_h}(\tilde{\boldsymbol{u}},\tilde{p}). \tag{48}$$

The modified Stokes projection is defined as $\mathbb{P}_{\gamma_h,0}^{X_h,Q_h}$. Hence, its properties can be established through the properties of $\mathbb{P}_{\gamma_h,\gamma_h}^{X_h,Q_h}$ and $\mathbb{P}_{\gamma_h,0}^{\boldsymbol{X},L^2}$. In order to study these two operators, we will repeatedly use Theorem 1.3 from [26] which can be presented as

Theorem 2. *Let $\boldsymbol{f} \in L^2$ and $g \in H^1 \cap Q$. Let $(\boldsymbol{u},p) \in \boldsymbol{X} \times Q$ such that*

$$\begin{cases} -\mu\Delta\boldsymbol{u} + \nabla p &= \boldsymbol{f}, \\ \nabla\cdot\boldsymbol{u} + \lambda p &= g, \end{cases} \tag{49}$$

where μ, λ are positive constants. Then $\boldsymbol{u} \in H^2$ and $p \in H^1$, and there exists a constant C that depends only on Ω such that

$$\mu\|u\|_{H^2} + (1+\mu\lambda)\|p\|_{H^1} \leq C\left(\|\boldsymbol{f}\|_{L^2} + \mu\|g\|_{H^1}\right). \tag{50}$$

4.2 Analysis of the operators

4.2.1 The penalty operator $\mathbb{P}^{\boldsymbol{X},L^2}_{\gamma_h,0}$

In this subsection, we establish convergence estimates for different norms.

Proposition 3. *Let $\boldsymbol{u} \in \boldsymbol{X}$ and $p \in Q$. Let us introduce $(\tilde{\boldsymbol{u}}, \tilde{p}) = \mathbb{P}^{\boldsymbol{X},L^2}_{\gamma_h,0}(\boldsymbol{u}, p)$. Then there exists a constant C independent of γ_h and Re such that*

$$\frac{1}{\sqrt{Re}}\|\boldsymbol{u} - \tilde{\boldsymbol{u}}\|_{H^1} + \sqrt{Re}\|p - \tilde{p}\|_{L^2} \leq \frac{C\gamma_h}{\sqrt{Re}}\|p\|_{L^2}. \tag{51}$$

Proof. From the definition of $\mathbb{P}^{\boldsymbol{X},L^2}_{\gamma_h,0}$, for any $(\boldsymbol{v}, q) \in \boldsymbol{X} \times L^2$, we infer that

$$a_{\gamma_h}\big((\tilde{\boldsymbol{u}}, \tilde{p}), (\boldsymbol{v}, q)\big) = a_{\gamma_h}\big((\boldsymbol{u}, p), (\boldsymbol{v}, q)\big) - \gamma_h\,(p, q)\,.$$

Using the coercivity of a_{γ_h}, we obtain

$$\begin{aligned} C'\|\boldsymbol{u} - \tilde{\boldsymbol{u}}, p - \tilde{p}\|^2_{\gamma_h} &\leq a_{\gamma_h}\big((\tilde{\boldsymbol{u}} - \boldsymbol{u}, \tilde{p} - p), (\tilde{\boldsymbol{u}} - \boldsymbol{u}, \tilde{p} - p)\big) \\ &\leq \gamma_h\,|(p, \tilde{p} - p)| \leq \gamma_h\|p\|_{L^2}\|\tilde{p} - p\|_{L^2}. \end{aligned} \tag{52}$$

Instead of directly applying Young's inequality, we want to replace the norm of $(\tilde{p} - p)$ by the one of $(\tilde{\boldsymbol{u}} - \boldsymbol{u})$. Using $(\boldsymbol{v}, 0)$ as a test function in the definition of $\mathbb{P}^{\boldsymbol{X},L^2}_{\gamma_h,0}$ yields:

$$\forall \boldsymbol{v} \in \boldsymbol{X}, \quad \frac{1}{Re}a(\tilde{\boldsymbol{u}} - \boldsymbol{u}, \boldsymbol{v}) + b(\boldsymbol{v}, \tilde{p} - p) = 0.$$

Using the LBB condition (25), we deduce that

$$\beta\|\tilde{p} - p\|_{L^2} \leq \sup_{\boldsymbol{v} \in \boldsymbol{X}\setminus\{0\}} \frac{b(\boldsymbol{v}, \tilde{p} - p)}{\|\boldsymbol{v}\|_{H^1}} = \sup_{\boldsymbol{v} \in \boldsymbol{X}\setminus\{0\}} \frac{a(\boldsymbol{u} - \tilde{\boldsymbol{u}}, \boldsymbol{v})}{\|\boldsymbol{v}\|_{H^1}} \leq \frac{A}{Re}\|\boldsymbol{u} - \tilde{\boldsymbol{u}}\|_{H^1}. \tag{53}$$

Using this inequality in (52) yields

$$\|\boldsymbol{u} - \tilde{\boldsymbol{u}}, p - \tilde{p}\|^2_{\gamma_h} \leq \frac{C\gamma_h}{Re}\|p\|_{L^2}\|\boldsymbol{u} - \tilde{\boldsymbol{u}}\|_{H^1} \leq \frac{C\gamma_h}{\sqrt{Re}}\|p\|_{L^2}\|\boldsymbol{u} - \tilde{\boldsymbol{u}}, p - \tilde{p}\|_{\gamma_h}, \tag{54}$$

which in turn implies that

$$\|\boldsymbol{u} - \tilde{\boldsymbol{u}}, p - \tilde{p}\|_{\gamma_h} \leq \frac{C\gamma_h}{\sqrt{Re}}\|p\|_{L^2}.$$

From this inequality, we obtain

$$\frac{1}{\sqrt{Re}}\|\boldsymbol{u} - \tilde{\boldsymbol{u}}\|_{H^1} \leq \frac{C\gamma_h}{\sqrt{Re}}\|p\|_{L^2}. \tag{55}$$

Inserting this inequality (55) in (53) yields

$$\sqrt{Re}\|\tilde{p} - p\|_{L^2} \leq \frac{A}{\beta\sqrt{Re}}\|\boldsymbol{u} - \tilde{\boldsymbol{u}}\|_{H^1} \leq \frac{C\gamma_h}{\sqrt{Re}}\|p\|_{L^2}, \tag{56}$$

and the desired result is finally obtained from (55) and (56). □

Proposition 4. *Let $\boldsymbol{u} \in \boldsymbol{X} \cap H^2$ and $p \in H^1 \cap Q$. Let us introduce $(\tilde{\boldsymbol{u}}, \tilde{p}) = \mathbb{P}^{\boldsymbol{X},L^2}_{\gamma_h,0}(\boldsymbol{u}, p)$. Then $\tilde{\boldsymbol{u}} \in H^2$, $\tilde{p} \in H^1 \cap Q$ and the following estimates hold, for C only depending on Ω:*

$$\|\tilde{\boldsymbol{u}}\|_{H^2} \leq C\left(\|\boldsymbol{u}\|_{H^2} + \gamma_h\|p\|_{H^1}\right), \tag{57}$$

$$\|\tilde{p}\|_{H^1} \leq C\|p\|_{H^1}, \tag{58}$$

$$\frac{1}{Re}\|\tilde{\boldsymbol{u}} - \boldsymbol{u}\|_{H^2} + \left(1 + \frac{\gamma_h}{Re}\right)\|\tilde{p} - p\|_{H^1} \leq \frac{C\gamma_h}{Re}\|p\|_{H^1}. \tag{59}$$

Proof. We start by proving (59). Owing to the definition of $\mathbb{P}^{\boldsymbol{X},L^2}_{\gamma_h,0}$, we have

$$\begin{cases} -\dfrac{1}{Re}\Delta\left(\tilde{\boldsymbol{u}}-\boldsymbol{u}\right)+\nabla\left(\tilde{p}-p\right) & =0, \\ \nabla\cdot\left(\tilde{\boldsymbol{u}}-\boldsymbol{u}\right)+\gamma_h\left(\tilde{p}-p\right) & =-\gamma_h p. \end{cases} \tag{60}$$

Applying Theorem 2 with $\mu=\frac{1}{Re}$ and $\lambda=\gamma_h$ yields (59).
From this inequality, we infer that

$$\begin{aligned} \|\tilde{\boldsymbol{u}}-\boldsymbol{u}\|_{H^2} &\leq C\gamma_h\|p\|_{H^1}, \\ \|\tilde{p}-p\|_{H^1} &\leq C\|p\|_{H^1}. \end{aligned}$$

Then (57) and (58) are obtained using triangular inequalities.

□

4.2.2 The projection operator $\mathbb{P}^{X_h,Q_h}_{\gamma_h,\gamma_h}$

Let us now turn our attention to the projection operator $\mathbb{P}^{X_h,Q_h}_{\gamma_h,\gamma_h}$.

Proposition 5. *Let $0\leqslant s\leqslant p_u$ and $0\leqslant s'\leqslant p_p$. Let $\boldsymbol{u}\in\boldsymbol{X}\cap H^{1+s}$ and $p\in H^{1+s'}\cap Q$. Let us introduce $(\boldsymbol{u}_h,p_h)=\mathbb{P}^{X_h,Q_h}_{\gamma_h,\gamma_h}(\boldsymbol{u},p)$. Then the following estimates hold, for C depending only on Ω:*

$$\|\boldsymbol{u}-\boldsymbol{u}_h,p-p_h\|^2_{\gamma_h}\leq\frac{C\,Re}{\gamma_h}\left(\frac{h^{2s}}{Re}\|\boldsymbol{u}\|^2_{H^{1+s}}+h^{2(1+s')}\gamma_h\|p\|^2_{H^{1+s'}}\right), \tag{61}$$

$$\|\boldsymbol{u}-\boldsymbol{u}_h\|^2_{L^2}\leq\frac{C\,Re^3}{\gamma_h^2}\left(\frac{h^{2(s+1)}}{Re}\|\boldsymbol{u}\|^2_{H^{1+s}}+h^{4+2s'}\gamma_h\|p\|^2_{H^{1+s'}}\right). \tag{62}$$

Proof. From the definition of the projection, for any $(\boldsymbol{v}_h,q_h)\in X_h\times Q_h$, we infer that

$$a_{\gamma_h}\big((\boldsymbol{u}-\boldsymbol{u}_h,p-p_h),(\boldsymbol{v}_h,q_h)\big)=0.$$

Using this Galerkin orthogonality and the continuity of a_{γ_h}, we obtain

$$a_{\gamma_h}\big((\boldsymbol{u}-\boldsymbol{u}_h,p-p_h),(\boldsymbol{u}-\boldsymbol{u}_h,p-p_h)\big)=a_{\gamma_h}\big((\boldsymbol{u}-\boldsymbol{u}_h,p-p_h),(\boldsymbol{u}-\mathcal{C}_h\boldsymbol{u},p-\mathcal{C}_hp)\big) \tag{63}$$

$$\leq\frac{C\sqrt{Re}}{\sqrt{\gamma_h}}\|\boldsymbol{u}-\boldsymbol{u}_h,p-p_h\|_{\gamma_h}\|\boldsymbol{u}-\mathcal{C}_h\boldsymbol{u},p-\mathcal{C}_hp\|_{\gamma_h}. \tag{64}$$

Using the definitions of the norm and a_{γ_h}, we also infer that

$$\|\boldsymbol{u}-\boldsymbol{u}_h,p-p_h\|^2_{\gamma_h}\leq Ca_{\gamma_h}\big((\boldsymbol{u}-\boldsymbol{u}_h,p-p_h),(\boldsymbol{u}-\boldsymbol{u}_h,p-p_h)\big).$$

As a result, we obtain

$$\|\boldsymbol{u}-\boldsymbol{u}_h,p-p_h\|^2_{\gamma_h}\leq\frac{C\sqrt{Re}}{\sqrt{\gamma_h}}\|\boldsymbol{u}-\boldsymbol{u}_h,p-p_h\|_{\gamma_h}\|\boldsymbol{u}-\mathcal{C}_h\boldsymbol{u},p-\mathcal{C}_hp\|_{\gamma_h}.$$

Using Young's inequality yields

$$\|\boldsymbol{u}-\boldsymbol{u}_h,p-p_h\|^2_{\gamma_h}\leq\frac{C\,Re}{\gamma_h}\|\boldsymbol{u}-\mathcal{C}_h\boldsymbol{u},p-\mathcal{C}_hp\|^2_{\gamma_h}.$$

which in turn implies that:

$$\|\boldsymbol{u}-\boldsymbol{u}_h,p-p_h\|^2_{\gamma_h}\leq\frac{2C\,Re}{\gamma_h}\left(\frac{1}{Re}\|\boldsymbol{u}-\mathcal{C}_h\boldsymbol{u}\|^2_{H^1}+\gamma_h\|p-\mathcal{C}_hp\|^2_{L^2}\right). \tag{65}$$

Using properties (32) of $\mathcal{C}_h$ yields (61).

The L^2 estimate is obtained using a Nitsche-Aubin argument. Let us define $\boldsymbol{w} \in \boldsymbol{X}$ and $r \in Q$ such that

$$\begin{cases} -\dfrac{1}{Re}\Delta \boldsymbol{w} + \nabla r & = \boldsymbol{u} - \boldsymbol{u}_h, \\ \nabla \cdot \boldsymbol{w} + \gamma_h r & = 0. \end{cases} \tag{66}$$

Since $\boldsymbol{u} - \boldsymbol{u}_h \in L^2$, we can apply Theorem 2 and we obtain $\boldsymbol{w} \in H^2$, $r \in H^1$ together with the estimate

$$\frac{1}{Re}\|w\|_{H^2} + \|r\|_{H^1} \leq C\|\boldsymbol{u} - \boldsymbol{u}_h\|_{L^2}. \tag{67}$$

Owing to the definition of $\boldsymbol{w}$ and r, we have, for any $\boldsymbol{v} \in \boldsymbol{X}$ and $q \in L^2$

$$a_{\gamma_h}\big((\boldsymbol{w}, r), (\boldsymbol{v}, q)\big) = (\boldsymbol{u} - \boldsymbol{u}_h, \boldsymbol{v})\,.$$

Let us use this identity for $\boldsymbol{v} = \boldsymbol{u} - \boldsymbol{u}_h$ and $q = p_h - p$. Then we obtain

$$\begin{aligned} \|\boldsymbol{u} - \boldsymbol{u}_h\|_{L^2}^2 &= a_{\gamma_h}\big((\boldsymbol{w}, r), (\boldsymbol{u} - \boldsymbol{u}_h, p_h - p)\big) \\ &= a_{\gamma_h}\big((\boldsymbol{u} - \boldsymbol{u}_h, p - p_h), (\boldsymbol{w}, -r)\big) \\ &= a_{\gamma_h}\big((\boldsymbol{u} - \boldsymbol{u}_h, p - p_h), (\boldsymbol{w} - \mathcal{C}_h w, \mathcal{C}_h r - r)\big). \end{aligned}$$

Owing to the continuity of a_{γ_h}, we deduce that

$$\|\boldsymbol{u} - \boldsymbol{u}_h\|_{L^2}^2 \leq \frac{C\sqrt{Re}}{\sqrt{\gamma_h}}\|\boldsymbol{u} - \boldsymbol{u}_h, p - p_h\|_{\gamma_h}\|\boldsymbol{w} - \mathcal{C}_h\boldsymbol{w}, r - \mathcal{C}_h r\|_{\gamma_h} \tag{68}$$

Let us estimate the term $\|\boldsymbol{w} - \mathcal{C}_h\boldsymbol{w}, r - \mathcal{C}_h r\|_{\gamma_h}$. From the definition of the norm and the properties of $\mathcal{C}_h$ (see (32)), we infer that

$$\|\boldsymbol{w} - \mathcal{C}_h\boldsymbol{w}, r - \mathcal{C}_h r\|_{\gamma_h} \leq Ch\left(\frac{1}{\sqrt{Re}}\|\boldsymbol{w}\|_{H^2} + \sqrt{\gamma_h}\|r\|_{H^1}\right).$$

Using the estimate (67) and $Re > 1$ leads to

$$\|\boldsymbol{w} - \mathcal{C}_h\boldsymbol{w}, r - \mathcal{C}_h r\|_{\gamma_h} \leq Ch\sqrt{Re}\|\boldsymbol{u} - \boldsymbol{u}_h\|_{L^2}.$$

Inserting this inequality in (68) yields

$$\|\boldsymbol{u} - \boldsymbol{u}_h\|_{L^2} \leq \frac{C\,Re\,h}{\sqrt{\gamma_h}}\|\boldsymbol{u} - \boldsymbol{u}_h, p - p_h\|_{\gamma_h}.$$

Taking the square of this inequality, together with (61) yields (62). □

Remark 3. *From (61) and (62), one can note that there exists a constant C independent of h, but depending on Ω and Re such that, for any $\boldsymbol{u} \in \boldsymbol{X} \cap H^2$ and $p \in H^1 \cap Q$,*

$$\begin{aligned} \|\boldsymbol{u} - \boldsymbol{u}_h\|_{H^1} &\leq C\frac{h}{\sqrt{\gamma_h}}\left(\|\boldsymbol{u}\|_{H^2} + \|p\|_{H^1}\right), \\ \|\boldsymbol{u} - \boldsymbol{u}_h\|_{L^2} &\leq C\frac{h^2}{\gamma_h}\left(\|\boldsymbol{u}\|_{H^2} + \|p\|_{H^1}\right). \end{aligned}$$

From interpolation theory, we obtain the estimate, for $0 \leq s \leq 1$:

$$\|\boldsymbol{u} - \boldsymbol{u}_h\|_{H^s} \leq C\left(\frac{h}{\sqrt{\gamma_h}}\right)^{2-s}\left(\|\boldsymbol{u}\|_{H^2} + \|p\|_{H^1}\right). \tag{69}$$

4.3 Error estimates for the operator $\mathbb{P}_{\gamma_h,0}^{X_h,Q_h}$

We now have all the tools at hand to prove an approximation result for the operator that we want to use.

Theorem 3. *Let $\boldsymbol{u} \in \boldsymbol{X} \cap H^2$ and $p \in H^1 \cap Q$. Let us introduce $(\boldsymbol{u}_h, p_h) = \mathbb{P}_{\gamma_h,0}^{X_h,Q_h}(\boldsymbol{u}, p)$. Then the following estimates hold, for C only depending on Ω:*

$$\|\boldsymbol{u} - \boldsymbol{u}_h, p - p_h\|_{\gamma_h}^2 \leq C \left(\frac{h^2}{\gamma_h} \|\boldsymbol{u}\|_{H^2}^2 + h^2 \gamma_h \|p\|_{H^1}^2 + Re\, h^2 \|p\|_{H^1}^2 + \frac{\gamma_h^2}{Re} \|p\|_{L^2}^2 \right), \tag{70}$$

$$\|\boldsymbol{u} - \boldsymbol{u}_h\|_{L^2}^2 \leq C \left(\frac{Re^2 h^4}{\gamma_h^2} \|\boldsymbol{u}\|_{H^2}^2 + \frac{Re^3 h^4}{\gamma_h} \|p\|_{H^1}^2 + \gamma_h^2 \|p\|_{L^2}^2 \right). \tag{71}$$

Proof. Let us introduce $(\tilde{\boldsymbol{u}}, \tilde{p}) = \mathbb{P}_{\gamma_h,0}^{\boldsymbol{X},L^2}(\boldsymbol{u}, p)$ so that we have $(\boldsymbol{u}_h, p_h) = \mathbb{P}_{\gamma_h,\gamma_h}^{X_h,Q_h}(\tilde{\boldsymbol{u}}, \tilde{p})$. We start from triangular inequalities to get

$$\|\boldsymbol{u} - \boldsymbol{u}_h, p - p_h\|_{\gamma_h}^2 \leq 2\|\boldsymbol{u} - \tilde{\boldsymbol{u}}, p - \tilde{p}\|_{\gamma_h}^2 + 2\|\tilde{\boldsymbol{u}} - \boldsymbol{u}_h, \tilde{p} - p_h\|_{\gamma_h}^2.$$

Let us now bound each term separately. From Proposition 3, we have the estimate

$$\|\boldsymbol{u} - \tilde{\boldsymbol{u}}, p - \tilde{p}\|_{\gamma_h}^2 \leq \frac{C\gamma_h^2}{Re} \|p\|_{L^2}^2.$$

For the second term, we use Proposition 5 with $s = 1$ and $s' = 0$ to obtain

$$\|\tilde{\boldsymbol{u}} - \boldsymbol{u}_h, \tilde{p} - p_h\|_{\gamma_h}^2 \leq \frac{CRe\, h^2}{\gamma_h} \left(\frac{1}{Re} \|\tilde{\boldsymbol{u}}\|_{H^2}^2 + \gamma_h \|\tilde{p}\|_{H^1}^2 \right).$$

From (57), we infer that

$$\|\tilde{\boldsymbol{u}} - \boldsymbol{u}_h, \tilde{p} - p_h\|_{\gamma_h}^2 \leq \frac{CRe\, h^2}{\gamma_h} \left(\frac{1}{Re} \|\boldsymbol{u}\|_{H^2}^2 + \frac{\gamma_h^2}{Re} \|p\|_{H^1}^2 + \gamma_h \|p\|_{H^1}^2 \right).$$

Thus we have the desired estimate

$$\|\boldsymbol{u} - \boldsymbol{u}_h, p - p_h\|_{\gamma_h}^2 \leq C \left(\frac{h^2}{\gamma_h} \|\boldsymbol{u}\|_{H^2}^2 + h^2 \gamma_h \|p\|_{H^1}^2 + Re\, h^2 \|p\|_{H^1}^2 + \frac{\gamma_h^2}{Re} \|p\|_{L^2}^2 \right).$$

We proceed similarly for the L^2 estimate, bounding $\|\tilde{\boldsymbol{u}} - \boldsymbol{u}_h\|_{L^2}$ using Proposition 5 and the error estimate (59), and bounding $\|\tilde{\boldsymbol{u}} - \boldsymbol{u}\|_{L^2}$ by $\sqrt{Re}\|\tilde{\boldsymbol{u}} - \boldsymbol{u}, \tilde{p} - p\|_{\gamma_h}$ and using (51). □

Remark 4. *Note that Eqns. (70)-(71) give a convergence result only if $\gamma_h \to 0$. The leading terms in (71) suggest to take $\gamma_h \sim Re^{1/2} h$, which would lead to order 1 in the L^2 norm, which is consistent with the results of the numerical simulations presented in Section 6.*

Remark 5. *We may need approximation results for the H^s norm, for $0 < s < 1$. There exists a constant C depending on Ω and Re, but not on h, such that*

$$\|\boldsymbol{u} - \boldsymbol{u}_h\|_{H^s}^2 \leq C \left(\frac{h^{4-2s}}{\gamma_h^{2-s}} \left(\|\boldsymbol{u}\|_{H^2}^2 + \|p\|_{H^1}^2 \right) + \gamma_h^2 \|p\|_{L^2}^2 \right). \tag{72}$$

This is obtained using the same decomposition as before, together with (69).

Let us end this section with a stability result.

Proposition 6. *Let $(\boldsymbol{u}, p) \in \boldsymbol{X} \times Q$ such that $\nabla \cdot \boldsymbol{u} = 0$. Let us introduce $(\boldsymbol{u}_h, p_h) = \mathbb{P}_{\gamma_h,0}^{X_h,Q_h}(\boldsymbol{u}, p)$. There exists C independent of $\boldsymbol{u}$ and p such that*

$$\|\boldsymbol{u} - \boldsymbol{u}_h\|_{H^1} \leq C \left(\|\boldsymbol{u}\|_{H^1} + \|p\|_{L^2} \right). \tag{73}$$

Proof. From the definition of $(\boldsymbol{u}_h, p_h)$ and the fact that $\nabla \cdot \boldsymbol{u} = 0$, we infer that

$$a_{\gamma_h}\left((\boldsymbol{u}_h, p_h), (\boldsymbol{u}_h, p_h)\right) = a_0\left((\boldsymbol{u}, p), (\boldsymbol{u}_h, p_h)\right) = \frac{1}{Re} a(\boldsymbol{u}, \boldsymbol{u}_h) + b(\boldsymbol{u}_h, p).$$

Owing to the coercivity of a_{γ_h} and the continuity of a and b, we deduce that

$$\frac{\alpha}{Re}\|\boldsymbol{u}_h\|_{H^1}^2 \leq C\|\boldsymbol{u}_h\|_{H^1}\left(\|\boldsymbol{u}\|_{H^1} + \|p\|_{L^2}\right).$$

Using the triangular inequality yields

$$\|\boldsymbol{u} - \boldsymbol{u}_h\|_{H^1} \leq \|\boldsymbol{u}\|_{H^1} + \|\boldsymbol{u}_h\|_{H^1} \leq C\left(\|\boldsymbol{u}\|_{H^1} + \|p\|_{L^2}\right).$$

□

5 Proof of Theorem 1

We are now able to prove Theorem 1, using the previously defined operator $\mathbb{P}_{\gamma_h,0}^{X_h,Q_h}$. Owing to the definition of φ_p^{n+1}, φ_u^{n+1}, η_p^{n+1}, η_u^{n+1}, summing (29)-(30) and subtracting (35)-(36) with corresponding test functions φ_p^{n+1}, φ_u^{n+1} yields:

$$\begin{aligned}
&(\delta_t\varphi_u^{n+1}, \varphi_u^{n+1}) + \frac{1}{Re}a(\varphi_u^{n+1}, \varphi_u^{n+1}) + \gamma_h(\varphi_p^{n+1}, \varphi_p^{n+1}) \\
&\qquad = (\delta_t\eta_u^{n+1}, \varphi_u^{n+1}) + \frac{1}{Re}a(\eta_u^{n+1}, \varphi_u^{n+1}) + b(\varphi_u^{n+1}, \eta_p^{n+1}) \\
&\qquad + c(\boldsymbol{u}^{n+1}, \boldsymbol{u}^{n+1}, \varphi_u^{n+1}) - c(\boldsymbol{u}_h^{n+1}, \boldsymbol{u}_h^{n+1}, \varphi_u^{n+1}) - \frac{Ra}{Re^2 Pr}(e_\theta^{n+1}\boldsymbol{e}_y, \varphi_u^{n+1}) \\
&\qquad + \left(R_u^{n+1}, \varphi_u^{n+1}\right) - b(\eta_u^{n+1}, \varphi_p^{n+1}) + \gamma_h(\eta_p^{n+1}, \varphi_p^{n+1}) - \gamma_h(p^{n+1}, \varphi_p^{n+1}) \\
&\qquad = (\delta_t\eta_u^{n+1}, \varphi_u^{n+1}) + a_{\gamma_h}\left((\eta_u^{n+1}, \eta_p^{n+1}), (\varphi_u^{n+1}, \varphi_p^{n+1})\right) \\
&\qquad + c(\boldsymbol{u}^{n+1}, \boldsymbol{u}^{n+1}, \varphi_u^{n+1}) - c(\boldsymbol{u}_h^{n+1}, \boldsymbol{u}_h^{n+1}, \varphi_u^{n+1}) - \frac{Ra}{Re^2 Pr}(e_\theta^{n+1}\boldsymbol{e}_y, \varphi_u^{n+1}) \\
&\qquad + \left(R_u^{n+1}, \varphi_u^{n+1}\right) - \gamma_h(p^{n+1}, \varphi_p^{n+1})
\end{aligned} \tag{74}$$

Owing to the definition of $\tilde{\boldsymbol{u}}_h^{n+1}$ and $\tilde{p}_h^{n+1}$, we obtain

$$\begin{aligned}
&a_{\gamma_h}\left((\eta_u^{n+1}, \eta_p^{n+1}), (\varphi_u^{n+1}, \varphi_p^{n+1})\right) - \gamma_h(p^{n+1}, \varphi_p^{n+1}) \\
&= a_0\left((\boldsymbol{u}^{n+1}, p^{n+1}), (\varphi_u^{n+1}, \varphi_p^{n+1})\right) - a_{\gamma_h}\left((\tilde{\boldsymbol{u}}_h^{n+1}, \tilde{p}_h^{n+1}), (\varphi_u^{n+1}, \varphi_p^{n+1})\right) = 0.
\end{aligned}$$

Thus, (74) simply reads

$$\begin{aligned}
&(\delta_t\varphi_u^{n+1}, \varphi_u^{n+1}) + \frac{1}{Re}a(\varphi_u^{n+1}, \varphi_u^{n+1}) + \gamma_h(\varphi_p^{n+1}, \varphi_p^{n+1}) \\
&\qquad = (\delta_t\eta_u^{n+1}, \varphi_u^{n+1}) + \left(R_u^{n+1}, \varphi_u^{n+1}\right) - \frac{Ra}{Re^2 Pr}(e_\theta^{n+1}\boldsymbol{e}_y, \varphi_u^{n+1}) \\
&\qquad + c(\boldsymbol{u}^{n+1}, \boldsymbol{u}^{n+1}, \varphi_u^{n+1}) - c(\boldsymbol{u}_h^{n+1}, \boldsymbol{u}_h^{n+1}, \varphi_u^{n+1}).
\end{aligned} \tag{75}$$

The left hand side of (75) is bounded from below by

$$\frac{1}{2\delta t}\left(\|\varphi_u^{n+1}\|_{L^2}^2 - \|\varphi_u^n\|_{L^2}^2 + \|\varphi_u^{n+1} - \varphi_u^n\|_{L^2}^2\right) + \frac{\alpha}{Re}\|\varphi_u^{n+1}\|_{H^1}^2 + \gamma_h\|\varphi_p^{n+1}\|_{L^2}^2$$

so we are left with the right hand side to bound from above. Using Young's inequality, we obtain

$$\left|(\delta_t \eta_u^{n+1}, \varphi_u^{n+1})\right| \leq \|\delta_t \eta_u^{n+1}\|_{L^2} \|\varphi_u^{n+1}\|_{L^2} \leq \frac{1}{2}\|\delta_t \eta_u^{n+1}\|_{L^2}^2 + \frac{1}{2}\|\varphi_u^{n+1}\|_{L^2}^2 \tag{76}$$

$$\left|(R_{\boldsymbol{u}}^{n+1}, \varphi_u^{n+1})\right| \leq \|R_{\boldsymbol{u}}^{n+1}\|_{L^2} \|\varphi_u^{n+1}\|_{L^2} \leq \frac{1}{2}\|R_{\boldsymbol{u}}^{n+1}\|_{L^2}^2 + \frac{1}{2}\|\varphi_u^{n+1}\|_{L^2}^2, \tag{77}$$

where κ_u and κ_p are some positive constants, independent of h, yet to be chosen.
The Boussinesq term is treated using the decomposition of e_θ^{n+1} :

$$\begin{aligned}\left|(e_\theta^{n+1}\boldsymbol{e}_y, \varphi_u^{n+1})\right| &\leq \|e_\theta^{n+1}\|_{L^2}\|\varphi_u^{n+1}\|_{L^2} \leq \left(\|\eta_\theta^{n+1}\|_{L^2} + \|\varphi_\theta^{n+1}\|_{L^2}\right)\|\varphi_u^{n+1}\|_{L^2} \\ &\leq \frac{1}{2}\|\eta_\theta^{n+1}\|_{L^2}^2 + \frac{1}{2}\|\varphi_\theta^{n+1}\|_{L^2}^2 + \|\varphi_u^{n+1}\|_{L^2}^2 \end{aligned} \tag{78}$$

The trilinear terms are treated using

$$\begin{aligned} & c(\boldsymbol{u}^{n+1}, \boldsymbol{u}^{n+1}, \varphi_u^{n+1}) - c(\boldsymbol{u}_h^{n+1}, \boldsymbol{u}_h^{n+1}, \varphi_u^{n+1}) \\ = \; & c(\boldsymbol{u}^{n+1}, \eta_u^{n+1}, \varphi_u^{n+1}) + c(\eta_u^{n+1}, \boldsymbol{u}^{n+1}, \varphi_u^{n+1}) - c(\eta_u^{n+1}, \eta_u^{n+1}, \varphi_u^{n+1}) \\ - \; & c(\varphi_u^{n+1}, \boldsymbol{u}^{n+1}, \varphi_u^{n+1}) + c(\varphi_u^{n+1}, \eta_u^{n+1}, \varphi_u^{n+1}) \end{aligned} \tag{79}$$

The first three terms are handled using (23)-(24) and a Young's inequality, for $0 < \sigma < 1$, and the last two are treated with (21) and the Young's inequality $xy \leq \frac{x^4}{4} + \frac{3y^{4/3}}{4}$:

$$\begin{aligned}\left|c(\boldsymbol{u}^{n+1}, \eta_u^{n+1}, \varphi_u^{n+1})\right| &\leq C\|\boldsymbol{u}^{n+1}\|_{H^1}\|\eta_u^{n+1}\|_{H^\sigma}\|\varphi_u^{n+1}\|_{H^1} \\ &\leq \frac{C^2}{4\kappa_u}\|\boldsymbol{u}^{n+1}\|_{H^1}^2\|\eta_u^{n+1}\|_{H^\sigma}^2 + \kappa_u\|\varphi_u^{n+1}\|_{H^1}^2, \end{aligned} \tag{80}$$

$$\begin{aligned}\left|c(\eta_u^{n+1}, \boldsymbol{u}^{n+1}, \varphi_u^{n+1})\right| &\leq C\|\boldsymbol{u}^{n+1}\|_{H^1}\|\eta_u^{n+1}\|_{H^\sigma}\|\varphi_u^{n+1}\|_{H^1} \\ &\leq \frac{C^2}{4\kappa_u}\|\boldsymbol{u}^{n+1}\|_{H^1}^2\|\eta_u^{n+1}\|_{H^\sigma}^2 + \kappa_u\|\varphi_u^{n+1}\|_{H^1}^2, \end{aligned} \tag{81}$$

$$\begin{aligned}\left|c(\eta_u^{n+1}, \eta_u^{n+1}, \varphi_u^{n+1})\right| &\leq C\|\eta_u^{n+1}\|_{H^1}^2\|\varphi_u^{n+1}\|_{H^1} \\ &\leq \frac{C^2}{4\kappa_u}\|\eta_u^{n+1}\|_{H^1}^4 + \kappa_u\|\varphi_u^{n+1}\|_{H^1}^2, \end{aligned} \tag{82}$$

$$\begin{aligned}\left|c(\varphi_u^{n+1}, \boldsymbol{u}^{n+1}, \varphi_u^{n+1})\right| &\leq C\|\varphi_u^{n+1}\|_{H^1}\|\boldsymbol{u}^{n+1}\|_{H^1}\|\varphi_u^{n+1}\|_{H^1}^{1/2}\|\varphi_u^{n+1}\|_{L^2}^{1/2} \\ &\leq C\|\boldsymbol{u}^{n+1}\|_{H^1}\|\varphi_u^{n+1}\|_{H^1}^{3/2}\|\varphi_u^{n+1}\|_{L^2}^{1/2} \\ &\leq \frac{C^4}{4\kappa_u^3}\|\boldsymbol{u}^{n+1}\|_{H^1}^4\|\varphi_u^{n+1}\|_{L^2}^2 + \frac{3\kappa_u}{4}\|\varphi_u^{n+1}\|_{H^1}^2, \end{aligned} \tag{83}$$

$$\begin{aligned}\left|c(\varphi_u^{n+1}, \eta_u^{n+1}, \varphi_u^{n+1})\right| &\leq C\|\varphi_u^{n+1}\|_{H^1}\|\eta_u^{n+1}\|_{H^1}\|\varphi_u^{n+1}\|_{H^1}^{1/2}\|\varphi_u^{n+1}\|_{L^2}^{1/2} \\ &\leq C\|\eta_u^{n+1}\|_{H^1}\|\varphi_u^{n+1}\|_{H^1}^{3/2}\|\varphi_u^{n+1}\|_{L^2}^{1/2} \\ &\leq \frac{C^4}{4\kappa_u^3}\mathcal{N}^4\|\varphi_u^{n+1}\|_{L^2}^2 + \frac{3\kappa_u}{4}\|\varphi_u^{n+1}\|_{H^1}^2. \end{aligned} \tag{84}$$

Note that for the last term, we used (73) to bound $\|\eta_u^{n+1}\|_{H^1}$. Gathering all these estimates leads to

$$\begin{aligned} & \frac{1}{2\delta t}\left(\|\varphi_u^{n+1}\|_{L^2}^2 - \|\varphi_u^n\|_{L^2}^2 + \|\varphi_u^{n+1} - \varphi_u^n\|_{L^2}^2\right) + \frac{\alpha}{Re}\|\varphi_u^{n+1}\|_{H^1}^2 + \gamma_h\|\varphi_p^{n+1}\|_{L^2}^2 \\ \leq \; & \frac{1}{2}\|R_{\boldsymbol{u}}^{n+1}\|_{L^2}^2 + \frac{1}{2}\|\delta_t\eta_u^{n+1}\|_{L^2}^2 + \frac{Re}{2Re^2Pr}\|\eta_\theta^{n+1}\|_{L^2}^2 + \frac{Ra}{2Re^2Pr}\|\varphi_\theta^{n+1}\|_{L^2}^2 \end{aligned} \tag{85}$$

$$+ \frac{9\kappa_u}{2}\|\varphi_u^{n+1}\|_{H^1}^2 + C_u'\|\varphi_u^{n+1}\|_{L^2}^2 + \frac{C^2}{4\kappa_u}\|\eta_u^{n+1}\|_{H^1}^4 + \frac{C^2}{2\kappa_u}\|\boldsymbol{u}^{n+1}\|_{H^1}\|\boldsymbol{u}^{n+1}\|_{H^\sigma}^2, \tag{86}$$

where $C'_u = 1 + \frac{Ra}{Re^2 Pr} + \frac{C^4}{2\kappa_u^3}\mathcal{N}^4$.
Choosing $\kappa_u = \frac{\alpha}{9Re}$, there exists C independent of h, such that

$$\begin{aligned}\frac{1}{2\delta t}\left(\|\varphi_u^{n+1}\|_{L^2}^2 - \|\varphi_u^n\|_{L^2}^2 + \|\varphi_u^{n+1} - \varphi_u^n\|_{L^2}^2\right) + \frac{\alpha}{2Re}\|\varphi_u^{n+1}\|_{H^1}^2 + \frac{\gamma}{2}\|\varphi_p^{n+1}\|_{L^2}^2 \\ \leq C\left(\|R_{\boldsymbol{u}}^{n+1}\|_{L^2}^2 + \|\delta_t\eta_u^{n+1}\|_{L^2}^2 + \|\eta_\theta^{n+1}\|_{L^2}^2 + \|\eta_u^{n+1}\|_{H^\sigma}^2 + \|\eta_u^{n+1}\|_{H^1}^4\right. \\ \left. + \|\varphi_\theta^{n+1}\|_{L^2}^2 + \|\varphi_u^{n+1}\|_{L^2}^2\right).\end{aligned} \tag{87}$$

We proceed similarly to get an estimate on the temperature, based on the approximation properties of $\mathcal{C}_h$.

$$\begin{aligned}\frac{1}{2\delta t}\left(\|\varphi_\theta^{n+1}\|_{L^2}^2 - \|\varphi_\theta^n\|_{L^2}^2 + \|\varphi_\theta^{n+1} - \varphi_\theta^n\|_{L^2}^2\right) + \frac{\bar{\alpha}K}{2Re\ Pr}\|\varphi_\theta^{n+1}\|_{H^1}^2 \\ \leq C\left(\|R_\theta^{n+1}\|_{L^2}^2 + \|\delta_t\eta_\theta^{n+1}\|_{L^2}^2 + \|\eta_\theta^{n+1}\|_{H^1}^2 + \|\varphi_\theta^{n+1}\|_{L^2}^2\right).\end{aligned} \tag{88}$$

Summing the last two estimates and removing some positive terms from the left hand side yields:

$$\begin{aligned}\frac{1}{2\delta t}\left(\|\varphi_u^{n+1}\|_{L^2}^2 - \|\varphi_u^n\|_{L^2}^2 + \|\varphi_\theta^{n+1}\|_{L^2}^2 - \|\varphi_\theta^n\|_{L^2}^2\right) \\ \leq C\Big(\|R_{\boldsymbol{u}}^{n+1}\|_{L^2}^2 + \|\delta_t\eta_u^{n+1}\|_{L^2}^2 + \|\eta_\theta^{n+1}\|_{L^2}^2 + \|\eta_u^{n+1}\|_{H^\sigma}^2 + \|\eta_u^{n+1}\|_{H^1}^4 \\ + \|R_\theta^{n+1}\|_{L^2}^2 + \|\delta_t\eta_\theta^{n+1}\|_{L^2}^2 + \|\eta_\theta^{n+1}\|_{H^1}^2 + \|\varphi_u^{n+1}\|_{L^2}^2 + \|\varphi_\theta^{n+1}\|_{L^2}^2\Big).\end{aligned} \tag{89}$$

Before applying Gronwall lemma, we want to bound all the terms in the right hand side (except for the last two), using the properties of $\mathcal{C}_h\theta$, $\tilde{\boldsymbol{u}}_h$, $\tilde{p}_h$. We first notice that

$$\begin{aligned}&\|R_{\boldsymbol{u}}^{n+1}\|_{L^2} \leq C\delta t\|\partial_{tt}\boldsymbol{u}\|_{L^\infty(L^2)}, && \|R_\theta^{n+1}\|_{L^2} \leq C\delta t\|\partial_{tt}\theta\|_{L^\infty(L^2)}, \\ &\|\eta_\theta^{n+1}\|_{L^2} \leq \|\eta_\theta^{n+1}\|_{H^1} \leq Ch^{s_\theta}\|\theta\|_{L^\infty(H^{1+s_\theta})}, && \|\delta_t\eta_\theta^{n+1}\|_{L^2} \leq Ch^{s_\theta}\|\partial_t\theta\|_{L^\infty(H^{s_\theta})}.\end{aligned}$$

Then, using the linearity of the operator $\mathbb{P}_{\gamma_h,0}^{X_h,Q_h}$ together with estimates (72) and (70), we infer that

$$\begin{aligned}\|\eta_u^{n+1}\|_{H^\sigma}^2 &\leq C\left(\frac{h^{4-2\sigma}}{\gamma_h^{2-\sigma}}\|\boldsymbol{u}\|_{L^\infty(H^2)}^2 + \frac{h^{4-\sigma}}{\gamma_h^{2-\sigma}}\|p\|_{L^\infty(H^1)}^2 + \gamma_h^2\|p\|_{L^\infty(L^2)}^2\right), \\ \|\eta_u^{n+1}\|_{H^1}^4 &\leq C\left(\frac{h^4}{\gamma_h^2}\|\boldsymbol{u}\|_{L^\infty(H^2)}^4 + \frac{h^4}{\gamma_h^2}\|p\|_{L^\infty(H^1)}^4 + \gamma_h^4\|p\|_{L^\infty(L^2)}^4\right), \\ \|\delta_t\eta_u^{n+1}\|_{L^2}^2 &\leq C\left(\frac{h^2}{\gamma_h}\|\delta_t\boldsymbol{u}^{n+1}\|_{H^2}^2 + \frac{h^2}{\gamma_h}\|\delta_t p^{n+1}\|_{H^1}^2 + \gamma_h^2\|\delta_t p^{n+1}\|_{L^2}^2\right), \\ &\leq C\left(\frac{h^2}{\gamma_h}\|\partial_t\boldsymbol{u}\|_{L^\infty(H^2)}^2 + \frac{h^2}{\gamma_h}\|\partial_t p\|_{L^\infty(H^1)}^2 + \gamma_h^2\|\partial_t p\|_{L^\infty(L^2)}^2\right).\end{aligned}$$

Owing to these estimates, we introduce the new quantity

$$\begin{aligned}E(\boldsymbol{u},p,\theta,\delta t,h,\gamma) := \delta t^2\|\partial_{tt}\boldsymbol{u}\|_{L^\infty(L^2)}^2 + \delta t^2\|\partial_{tt}\theta\|_{L^\infty(L^2)}^2 + h^{2s_\theta}\|\theta\|_{L^\infty(H^{1+s_\theta})}^2 \\ + h^{2s_\theta}\|\partial_t\theta\|_{L^\infty(H^{s_\theta})}^2 + \frac{h^{4-2\sigma}}{\gamma_h^{2-\sigma}}\|\boldsymbol{u}\|_{L^\infty(H^2)}^2 + \frac{h^{4-\sigma}}{\gamma_h^{2-\sigma}}\|p\|_{L^\infty(H^1)}^2 \\ + \gamma_h^2\|p\|_{L^\infty(L^2)}^2 + \frac{h^4}{\gamma_h^2}\|\boldsymbol{u}\|_{L^\infty(H^2)}^4 + \frac{h^4}{\gamma_h^2}\|p\|_{L^\infty(H^1)}^4 \\ + \gamma_h^4\|p\|_{L^\infty(L^2)}^4 + \frac{h^2}{\gamma_h}\|\partial_t\boldsymbol{u}\|_{L^\infty(H^2)}^2 + \frac{h^2}{\gamma_h}\|\partial_t p\|_{L^\infty(H^1)}^2 + \gamma_h^2\|\partial_t p\|_{L^\infty(L^2)}^2,\end{aligned}$$

so that (89) yields

$$\frac{1}{\delta t}\left(\|\varphi_u^{n+1}\|_{L^2}^2 - \|\varphi_u^n\|_{L^2}^2 + \|\varphi_\theta^{n+1}\|_{L^2}^2 - \|\varphi_\theta^n\|_{L^2}^2\right) \tag{90}$$

$$\leq C\left(E(\boldsymbol{u}, p, \theta, \delta t, h, \gamma) + \|\varphi_\theta^{n+1}\|_{L^2}^2 + \|\varphi_u^{n+1}\|_{L^2}^2\right). \tag{91}$$

Finally, we use the discrete Gronwall lemma, and we obtain the desired estimate, provided we choose $\boldsymbol{u}_h^0$ and θ_h^0 such that $\varphi_u^0 = 0$ and $\varphi_\theta^0 = 0$.

6 Numerical results

In this section, we present numerical results to support theoretical estimates. It is worth mentioning that we performed the tests on domains that are not of class $C^{1,1}$. We start by illustrating (70) and (71) before turning our attention to the natural convection problem. We also illustrate the gain in computational cost allowed by the use of the linear element instead of the standard Taylor-Hood elements. All simulations are performed using the open-source software FreeFem++ [27, 28].

6.1 The modified projection $\mathbb{P}_{\gamma_h,0}^{X_h,Q_h}$

Given $(\boldsymbol{u}, p)$, we compute $(\tilde{\boldsymbol{u}}_{\boldsymbol{h}}, \tilde{p}_h) \in X_h \times Q_h$ such that

$$\forall (\boldsymbol{v}_h, q_h) \in X_h \times Q_h, \qquad a_{\gamma_h}\big((\tilde{\boldsymbol{u}}_{\boldsymbol{h}}, \tilde{p}_h), (\boldsymbol{v}_h, q_h)\big) = a_0\big((\boldsymbol{u}, p), (\boldsymbol{v}_h, q_h)\big). \tag{92}$$

We want to illustrate the results of Theorem 3. The results for the P_1-P_1 elements (i.e. $p_u = p_p = 1$) are better than expected. Therefore, we also performed simulations using P_1-P_0 elements, in order to illustrate the sharpness of our error estimates (70)-(71). The choice of γ_h modifies the estimates and consequently the order of convergence. Different values of γ_h are tested to reach the best estimate. We present some numerical results for the following values of γ_h:

- $\gamma_h = 10^{-7}$, which is not supposed to yield any convergence, neither for the velocity nor the pressure;
- $\gamma_h = Re^{1/3}h^{2/3}$, which is the best choice for the convergence of velocity in the H^1 norm: this should yield convergence of order $2/3$ for the velocity (L^2 and H^1 norms) and order $1/3$ for the pressure;
- $\gamma_h = Re^{1/2}h$, which is the best choice for the convergence of velocity in the L^2 norm: this should yield convergence for the velocity of order 1 in the L^2 norm, order $1/2$ in the H^1 norm, but no convergence in pressure;
- $\gamma_h = Re\, h^2$, which is not supposed to yield any convergence, and even explosion for the pressure.

6.1.1 Steady Burggraf flow (case `MP-Bur`)

We first focus on the Burggraf manufactured solution, see [1]. This case is a time-independent recirculating flow inside a square cavity $[0,1] \times [0,1]$. It is similar to the well-known lid driven cavity flow, but the velocity singularity at the top corners of the cavity is avoided. The exact solution of the flow is:

$$\begin{aligned} u_1(x,y) &= \chi g'(x)h'(y), \\ u_2(x,y) &= -\chi g''(x)h(y), \\ p(x,y) &= \tilde{p}(x,y) - \frac{1}{|\Omega|}\int_\Omega \tilde{p}(x,y), \end{aligned} \tag{93}$$

with $\chi > 0$ is a scaling parameter and functions and the function $\tilde{p}$, g and h are defined by:

$$\begin{aligned} \tilde{p}(x,y) &= \frac{\chi}{Re}\left(h^{(3)}(y)g(x) + g''(x)h'(y)\right) + \frac{\chi^2}{2}g'(x)^2\left(h(y)h''(y) - h'(y)^2\right) \\ g(x) &= \frac{x^5}{5} - \frac{x^4}{2} + \frac{x^3}{3}, \\ h(y) &= y^4 - y^2. \end{aligned} \tag{94}$$

Note that the velocity at the top border of the cavity is:

$$u_1(x,1) = 2\chi(x^4 - 2x^3 + x^2), \quad u_2(x,1) = 0, \tag{95}$$

which ensures the continuity of the velocity at the corners ($\boldsymbol{u}(0,1) = \boldsymbol{u}(1,1) = 0$), since non-slip walls are imposed for the other borders: $\boldsymbol{u}(x,0) = \boldsymbol{u}(0,y) = \boldsymbol{u}(1,y) = 0$. The Reynolds number Re is taken equal to 1 and χ equal to 8.

In all the tables, the column "rate" reports the computed order of convergence based on the computed errors. Empty cells mean that the iterative solver did not converge.

	$\gamma_h \sim 10^{-7}$		$\gamma_h \sim Re^{1/3}h^{2/3}$		$\gamma_h \sim Re^{1/2}h$		$\gamma_h \sim Re\,h^2$	
h	err	rate	err	rate	err	rate	err	rate
1/20	4.42E-03		5.27E-02		2.32E-02		3.92E-03	
1/40	1.14E-03	1.95	3.63E-02	0.54	1.21E-02	0.94	1.01E-03	1.96
1/80	2.93E-04	1.96	2.44E-02	0.57	6.25E-03	0.96	2.58E-04	1.97
1/160	7.44E-05	1.98	1.61E-02	0.60	3.17E-03	0.98	6.55E-05	1.98
1/200	4.78E-05	1.98	1.40E-02	0.62	2.54E-03	0.99	4.21E-05	1.98

Table 1: Case `MP-Bur` *:* $\|\boldsymbol{u} - \boldsymbol{u}_h\|_{L^2}$ *for* P_1*-*P_1 *elements.*

	$\gamma_h \sim 10^{-7}$		$\gamma_h \sim Re^{1/3}h^{2/3}$		$\gamma_h \sim Re^{1/2}h$		$\gamma_h \sim Re\,h^2$	
h	err	rate	err	rate	err	rate	err	rate
1/20	2.09E+05		4.38E-01		5.01E-01		8.45E+00	
1/40	5.49E+04	1.93	2.97E-01	0.56	2.82E-01	0.83	8.91E+00	-0.08
1/80	1.41E+04	1.96	2.00E-01	0.57	1.56E-01	0.85	9.15E+00	-0.04
1/160	3.56E+03	1.98	1.32E-01	0.59	8.57E-02	0.86	9.27E+00	-0.02
1/200	2.29E+03	1.99	1.16E-01	0.61	7.08E-02	0.86	9.30E+00	-0.01

Table 2: Case `MP-Bur` *:* $\|\boldsymbol{p} - \boldsymbol{p}_h\|_{L^2}$ *for* P_1*-*P_1 *element*

	$\gamma_h \sim 10^{-7}$		$\gamma_h \sim Re^{1/3}h^{2/3}$		$\gamma_h \sim Re^{1/2}h$		$\gamma_h \sim Re\,h^2$	
h	err	rate	err	rate	err	rate	err	rate
1/20	3.11E-01		3.57E-01		2.79E-01		2.85E-01	
1/40	1.59E-01	0.97	2.16E-01	0.72	1.41E-01	0.98	1.45E-01	0.97
1/80	8.09E-02	0.98	1.35E-01	0.68	7.09E-02	0.99	7.37E-02	0.98
1/160	4.08E-02	0.99	8.48E-02	0.67	3.55E-02	1.00	3.71E-02	0.99
1/200	3.27E-02	0.99	7.32E-02	0.66	2.84E-02	1.00	2.97E-02	0.99

Table 3: Case `MP-Bur` *:* $\|\boldsymbol{u} - \boldsymbol{u}_h\|_{H^1}$ *for* P_1*-*P_1 *element*

We note from Tables 1-2-3 that (P_1-P_1) elements give the expected behaviour for $\gamma_h \sim Re^{1/3}h^{2/3}$ and $\gamma_h \sim Re^{1/2}h$. Nevertheless, we find a better performance than expected for $\gamma_h \sim 10^{-7}$ and $\gamma_h \sim Re\ h^2$. However, the predicted behaviour from Theorem 3 is recovered with (P_1-P_0) elements, see Tables 4-5-6.

	$\gamma_h \sim 10^{-7}$		$\gamma_h \sim Re^{1/3}h^{2/3}$		$\gamma_h \sim Re^{1/2}h$		$\gamma_h \sim Re\,h^2$	
h	err	rate	err	rate	err	rate	err	rate
1/20	1.52E-01		5.39E-02		2.88E-02		9.09E-02	
1/40	1.53E-01	-0.01	3.66E-02	0.56	1.45E-02	0.99	9.10E-02	0.00
1/80	1.53E-01	0.00	2.45E-02	0.58	7.30E-03	0.99	9.11E-02	0.00
1/160	1.53E-01	0.00	1.61E-02	0.60	3.67E-03	0.99	9.11E-02	0.00
1/200			1.40E-02	0.62	2.94E-03	1.00		

Table 4: Case `MP-Bur` *:* $\|\boldsymbol{u} - \boldsymbol{u}_h\|_{L^2}$ *for* P_1-P_0 *element*

	$\gamma_h \sim 10^{-7}$		$\gamma_h \sim Re^{1/3}h^{2/3}$		$\gamma_h \sim Re^{1/2}h$		$\gamma_h \sim Re\,h^2$	
h	err	rate	err	rate	err	rate	err	rate
1/20	1.27E+06		1.22E+00		3.06E+00		5.26E+01	
1/40	6.39E+05	0.99	9.76E-01	0.32	3.15E+00	-0.04	1.06E+02	-1.01
1/80	3.20E+05	1.00	7.72E-01	0.34	3.19E+00	-0.02	2.12E+02	-1.00
1/160	1.60E+05	1.00	6.09E-01	0.34	3.22E+00	-0.01	4.24E+02	-1.00
1/200			5.64E-01	0.34	3.22E+00	-0.01		

Table 5: Case `MP-Bur` *:* $\|\boldsymbol{p} - \boldsymbol{p}_h\|_{L^2}$ *for* P_1-P_0 *element*

	$\gamma_h \sim 10^{-7}$		$\gamma_h \sim Re^{1/3}h^{2/3}$		$\gamma_h \sim Re^{1/2}h$		$\gamma_h \sim Re\,h^2$	
h	err	rate	err	rate	err	rate	err	rate
1/20	1.46E+00		3.60E-01		3.07E-01		9.04E-01	
1/40	1.47E+00	0.00	2.17E-01	0.73	1.58E-01	0.96	8.93E-01	0.02
1/80	1.47E+00	0.00	1.35E-01	0;69	8.04E-02	0.98	8.91E-01	0.00
1/160	1.46E+00	0.00	8.49E-02	0.67	4.05E-02	0.99	8.90E-01	0.00
1/200			7.32E-02	0.66	3.24E-02	0.99		

Table 6: Case `MP-Bur` *:* $\|\boldsymbol{u} - \boldsymbol{u}_h\|_{H^1}$ *for* P_1-P_0 *element*

6.1.2 Steady natural convection (case `MP-NC`)

The first test case `MP-Bur` is an academic validation, on a regular manufactured solution. We also assess the accuracy of the modified Stokes projection on a more realistic case.

To do so, we consider the classical problem of the thermally driven square cavity $[0,1] \times [0,1]$, filled with air, described by the system of equations (1)-(3). The left wall is kept at a constant hot temperature $\theta_h = 0.5$ and the right wall is kept at a constant cold temperature $\theta_c = -0.5$. Top and bottom walls are adiabatic. Natural convection flow is computed for the Rayleigh number $Ra = 10^4$. The Prandtl number is set to $Pr = 0.71$ and the Reynolds number to $Re = \sqrt{\frac{Ra}{Pr}}$.

We compute a reference solution with (P_2-P_1-P_2) finite elements for the velocity, pressure and temperature on a fine fixed grid with mesh size $h = 1/500$. γ_h is taken equal to 0. The non linear system (29)-(31) is solved using a

Newton algorithm. The initial state consists of motionless air ($\boldsymbol{u} = 0$), with a linear distribution of the temperature. For the time integration, we use a second-order Gear (BDF2) scheme and set $\delta t = h$. It has been proven in [7] that this choice ensures convergence. Therefore, we use this result as reference solution.

The computations are performed until a steady state is reached. Then we use the computed $(\boldsymbol{u}, p)$ in the right hand side of (92). The results are similar to the results for Case `MP-Bur` and still in agreement with theoretical estimates. Since the results are similar, we only present the L^2 error on the velocity and the L^2 error on the pressure in Tables 7-8 (P_1-P_1) and Tables 9-10 (P_1-P_0).

	$\gamma_h \sim 10^{-7}$		$\gamma_h \sim Re^{1/3}h^{2/3}$		$\gamma_h \sim Re^{1/2}h$		$\gamma_h \sim Re\,h^2$	
h	err	rate	err	rate	err	rate	err	rate
1/20	6.86E-03		4.19E-02		3.51E-02		6.31E-03	
1/40	1.72E-03	2.00	2.77E-02	0.59	1.86E-02	0.92	1.60E-03	1.98
1/80	4.28E-04	2.00	1.81E-02	0.62	9.56E-03	0.96	4.01E-04	2.00
1/160	1.07E-04	2.00	1.16E-02	0.64	4.85E-03	0.98	1.00E-04	2.00
1/320			7.42E-03	0.65	2.44E-03	0.99		

Table 7: Case `MP-NC` : $\|\boldsymbol{u} - \boldsymbol{u}_h\|_{L^2}$ for P_1-P_1-element

	$\gamma_h \sim 10^{-7}$		$\gamma_h \sim Re^{1/3}h^{2/3}$		$\gamma_h \sim Re^{1/2}h$		$\gamma_h \sim Re\,h^2$	
h	err	rate	err	rate	err	rate	err	rate
1/20	7.33E+00		6.94E-03		6.53E-03		1.43E-02	
1/40	2.31E+00	1.66	4.15E-03	0.74	3.50E-03	0.90	1.36E-02	0.08
1/80	1.25E+00	0.89	2.51E-03	0.73	1.84E-03	0.93	1.33E-02	0.03
1/160	1.25E+00	0.00	1.54E-03	0.71	9.58E-04	0.94	1.31E-02	0.01
1/320			9.49E-04	0.69	5.01E-04	0.93		

Table 8: Case `MP-NC` : $\|\boldsymbol{p} - \boldsymbol{p}_h\|_{L^2}$ for P_1-P_1-element

	$\gamma_h \sim 10^{-7}$		$\gamma_h \sim Re^{1/3}h^{2/3}$		$\gamma_h \sim Re^{1/2}h$		$\gamma_h \sim Re\,h^2$	
h	err	rate	err	rate	err	rate	err	rate
1/20	1.35E-01		4.27E-02		3.71E-02		8.78E-02	
1/40	1.35E-01	0.00	2.80E-02	0.61	1.99E-02	0.90	8.78E-02	0.00
1/80	1.35E-01	0.00	1.81E-02	0.63	1.03E-02	0.95	8.78E-02	0.00
1/160	1.35E-01	0.00	1.16E-02	0.64	5.23E-03	0.97	8.78E-02	0.00
1/320			7.43E-03	0.65	2.64E-03	0.99		

Table 9: Case `MP-NC` : $\|\boldsymbol{u} - \boldsymbol{u}_h\|_{L^2}$ for P_1-P_0-element

	$\gamma_h \sim 10^{-7}$		$\gamma_h \sim Re^{1/3}h^{2/3}$		$\gamma_h \sim Re^{1/2}h$		$\gamma_h \sim Re\,h^2$	
h	err	rate	err	rate	err	rate	err	rate
1/20	7.49E+01		1.33E-02		1.49E-02		9.23E-02	
1/40	4.44E+01	0.75	1.05E-02	0.34	1.48E-02	0.00	1.88E-01	-1.03
1/80	3.58E+01	0.31	8.32E-03	0.33	1.53E-02	-0.05	3.79E-01	-1.01
1/160	1.43E+01	1.32	6.62E-03	0.33	1.58E-02	-0.04	7.59E-01	-1.00
1/320			5.26E-03	0.33	1.60E-02	-0.02		

Table 10: Case `MP-NC` *:* $\|\boldsymbol{p} - \boldsymbol{p}_h\|_{L^2}$ *for* P_1*-*P_0*-element*

As a result, even though (P_1-P_1) elements give better results than expected, the numerical results are in accordance with our error estimates. These estimates seems to be sharp since the predicted rates are recovered for (P_1-P_0) elements.

6.2 Natural convection in 2D

The convergence of our operator being assessed, we can illustrate the convergence properties for the natural convection problem. Note that in numerical simulations, we used a second order discretization in time, which only improves the accuracy with respect to δt. The remaining of the estimate (44) still holds.

As for the modified projection, we illustrate Corollary 1 on two examples. The first one consists of a manufactured solution, see [29]. The second example is a physical case of natural convection, compared to the reference solution described in Section 6.1.2. A second validation is obtained by comparing the vertical velocity profile at mid-domain ($y = 0.5$) to a spectral approximation [30].

Leading terms	γ_h	expected order
$\delta t, h^2, \frac{h^{4-\sigma}}{\gamma_h^{2-\sigma}}, \gamma_h^2$	10^{-7}	Stability
	$Re^{1/3}h^{2/3}$	Convergence with an order 2/3
	$Re^{1/2}h$	Convergence with an order 1
	$Re\,h^2$	Stability

Table 11: Expected order of convergence for $\|u - u_h\|_{L^2}$ *and* $\|\theta - \theta_h\|_{L^2}$

6.2.1 Manufactured solution (case `NC-Nour`)

We first consider the manufactured time-dependent solution suggested in [29]:

$$\begin{aligned} u_1(x,y,t) &= (\delta U_0 + \alpha_u \sin(t))\, \cos(x+\gamma_1 t)\, \sin(y+\gamma_2 t), \\ u_2(x,y,t) &= -(\delta U_0 + \alpha_u \sin(t))\, \sin(x+\gamma_1 t)\, \cos(y+\gamma_2 t), \\ \theta(x,y,t) &= \bar{\theta} + (\delta\theta_0 + \alpha_t \sin(t))\, \cos(x+\gamma_1 t)\, \sin(y+\gamma_2 t), \\ p(x,y,t) &= \bar{P} + (\delta P_0 + \alpha_p \sin(t))\, \sin(x+\gamma_1 t)\, \cos(y+\gamma_2 t), \end{aligned} \tag{96}$$

The values of the constants are reported in Table 12. The corresponding source terms are:

γ_1	γ_2	$\bar{P}$	$\bar{\theta}$	δP_0	$\delta\theta_0$	δU_0	α_p	α_u	α_t
0.1	0.1	0	1.0	0.1	1.0	1.0	0.05	0.4	0.1

Table 12: Parameters for case `NC-Nour` (96).

$$
\begin{aligned}
f_{u_1} &= \alpha_u\,\cos(t)\,\cos(a)\sin(b) - U_c\,\gamma_1\,\sin(a)\sin(b) + U_c\,\gamma_2\,\cos(a)\cos(b) \\
&\quad -U_c\,u_1(x,y,t)\,\sin(a)\sin(b) + U_c\,u_2(x,y,t)\,\cos(a)\cos(b) + P_c\,\cos(a)\cos(b) \\
&\quad +\frac{2}{Re}\,u_1(x,y,t), \\
f_{u_2} &= -\alpha_u\,\cos(t)\,\sin(a)\cos(b) - U_c\,\gamma_1\,\cos(a)\cos(b) + U_c\,\gamma_2\,\sin(a)\sin(b) \\
&\quad -U_c\,u_1(x,y,t)\,\cos(a)\cos(b) + U_c\,u_2(x,y,t)\,\sin(a)\sin(b) - P_c\,\sin(a)\,\sin(b) \\
&\quad +\frac{2}{Re}\,u_2(x,y,t) - \frac{Ra}{PrRe^2}\,T(x,y,t), \\
f_\theta &= \alpha_t\,\cos(t)\,\cos(a)\sin(b) - \theta_c\,\gamma_1\,\sin(a)\sin(b) + \theta_c\,\gamma_2\,\cos(a)\cos(b) \\
&\quad -\theta_c\,u_1(x,y,t)\,\sin(a)\sin(b) + \theta_c\,u_2(x,y,t)\,\cos(a)\cos(b) + \frac{2K}{RePr}\,\theta_c\,\cos(a)\sin(b),
\end{aligned}
\tag{97}
$$

where $a = (x+\gamma_1 t)$, $b = (y+\gamma_2 t)$ and $U_c = (\delta U_0 + \alpha_u \sin(t))$, $\theta_c = (\delta\theta_0 + \alpha_u \sin(t))$, $P_c = (\delta P_0 + \alpha_u \sin(t))$. We want to assess the accuracy of our estimates with respect to h. Since we use a second order scheme in time, we choose $\delta t \simeq h$. Dimensionless parameters are chosen to emulate the convection of air, with a Rayleigh number $Ra = 10^6$, a Prandtl number $Pr = 0.71$ and Reynolds number $Re = \sqrt{Ra/Pr}$. The errors are computed at the final time $t_f = \pi/2$.

	$\gamma_h \sim 10^{-7}$		$\gamma_h \sim Re^{1/3}h^{2/3}$		$\gamma_h \sim Re^{1/2}h$		$\gamma_h \sim Re\,h^2$	
h	err	rate	err	rate	err	rate	err	rate
1/20	8.79E-04		1.49E-02		1.71E-02		2.48E-02	
1/40	2.15E-04	2.03	9.89E-03	0.59	9.48E-03	0.85	8.31E-03	1.58
1/80	5.25E-05	2.03	6.48E-03	0.61	4.99E-03	0.93	2.22E-03	1.90
1/160	1.30E-05	2.01	4.19E-03	0.63	2.56E-03	0.96	5.64E-04	1.98
1/320			2.69E-03	0.64	1.30E-03	0.98	1.42E-04	1.99

Table 13: Case `NC-Nour` *:* $\|\boldsymbol{u} - \boldsymbol{u}_h\|_{L^2}$ *for* P_1-P_1-P_1 *element*

	$\gamma_h \sim 10^{-7}$		$\gamma_h \sim Re^{1/3}h^{2/3}$		$\gamma_h \sim Re^{1/2}h$		$\gamma_h \sim Re\,h^2$	
h	err	rate	err	rate	err	rate	err	rate
1/20	1.38E-03		4.57E-03		5.25E-03		8.16E-03	
1/40	3.37E-04	2.03	2.41E-03	0.92	2.31E-03	1.19	2.03E-03	2.01
1/80	8.47E-05	1.99	1.47E-03	0.71	1.14E-03	1.02	5.31E-04	1.94
1/160	2.12E-05	2.00	9.34E-04	0.66	5.75E-04	0.99	1.35E-04	1.98
1/320			5.93E-04	0.65	2.88E-04	0.99	3.38E-05	2.00

Table 14: Case `NC-Nour` *:* $\|\theta - \theta_h\|_{L^2}$ *for* P_1-P_1-P_1 *element*

	$\gamma_h \sim 10^{-7}$		$\gamma_h \sim Re^{1/3}h^{2/3}$		$\gamma_h \sim Re^{1/2}h$		$\gamma_h \sim Re\,h^2$	
h	err	rate	err	rate	err	rate	err	rate
1/20	1.51E+04		6.81E-03		8.07E-03		1.44E-02	
1/40	3.81E+03	1.99	4.71E-03	0.53	4.51E-03	0.84	3.96E-03	1.87
1/80	9.52E+02	2.00	2.81E-03	0.74	2.17E-03	1.06	1.09E-03	1.86
1/160	2.38E+02	2.00	1.70E-03	0.73	1.04E-03	1.06	5.27E-04	1.05
1/320			1.05E-03	0.70	5.11E-04	1.03	5.25E-04	0.01

Table 15: Case `NC-Nour` *:* $\|\boldsymbol{p} - \boldsymbol{p}_h\|_{L^2}$ *for* P_1-P_1-P_1 *element*

Since the error estimate of natural convection involves the error estimates of modified projection, we observe the same behaviour as before i.e. the (P_1-P_1) finite elements seem to yield a better convergence rate than expected. However, these results are in good agreement with our estimates. In particular, the correct convergence rates for the velocity and temperature are observed for $\gamma_h = Re^{1/3}h^{2/3}$ and $\gamma_h = Re^{1/2}h$ and the case $\gamma_h = 10^{-7}$ yields computational issues for small values of h.

6.2.2 Natural convection in a square (case `NC-Sq`)

We are now interested in a physical case. We consider here the reference solution described in Section 6.1.2. We numerically solve equations describing the classical natural convection with a finite element scheme (P_1-P_1-P_1) and we compare our results to this reference solution. The Rayleigh number is taken as $Ra = 10^4$, the Prandtl number $Pr = 0.71$ and the Reynolds number is $Re = \sqrt{Ra/Pr}$. The results are presented in Tables 16-17-18.

	$\gamma_h \sim 10^{-7}$		$\gamma_h \sim Re^{1/3}h^{2/3}$		$\gamma_h \sim Re^{1/2}h$		$\gamma_h \sim Re\,h^2$	
h	err	rate	err	rate	err	rate	err	rate
1/20	5.57E-03		1.15E-02		6.08E-03		5.28E-03	
1/40	1.39E-03	2.00	7.00E-03	0.71	2.34E-03	1.38	1.34E-03	1.98
1/80	3.47E-04	2.00	4.43E-03	0.66	1.08E-03	1.12	3.36E-04	1.99
1/160	8.68E-05	2.00	2.81E-03	0.66	5.30E-04	1.03	8.50E-05	1.98
1/320	3.23E-05	1.43	8.09E-04	1.80	2.65E-04	1.00	3.21E-05	1.40

Table 16: Case `NC-Sq` *:* $\|\boldsymbol{u} - \boldsymbol{u}_h\|_{L^2}$ *for* P_1-P_1-P_1 *elements*

	$\gamma_h \sim 10^{-7}$		$\gamma_h \sim Re^{1/3}h^{2/3}$		$\gamma_h \sim Re^{1/2}h$		$\gamma_h \sim Re\,h^2$	
h	err	rate	err	rate	err	rate	err	rate
1/20	4.33E-03		1.76E-02		8.86E-03		6.59E-03	
1/40	1.08E-03	2.01	1.04E-02	0.76	3.65E-03	1.28	1.67E-03	1.98
1/80	2.74E-04	1.97	6.42E-03	0.69	1.66E-03	1.14	4.24E-04	1.98
1/160	1.00E-04	1.45	4.06E-03	0.66	8.21E-04	1.01	1.41E-04	1.58
1/320	5.54E-05	0.86	1.20E-03	1.76	4.25E-04	0.95	6.70E-05	1.08

Table 17: Case `NC-Sq` *:* $\|\theta - \theta_h\|_{L^2}$ *for* P_1-P_1-P_1 *elements*

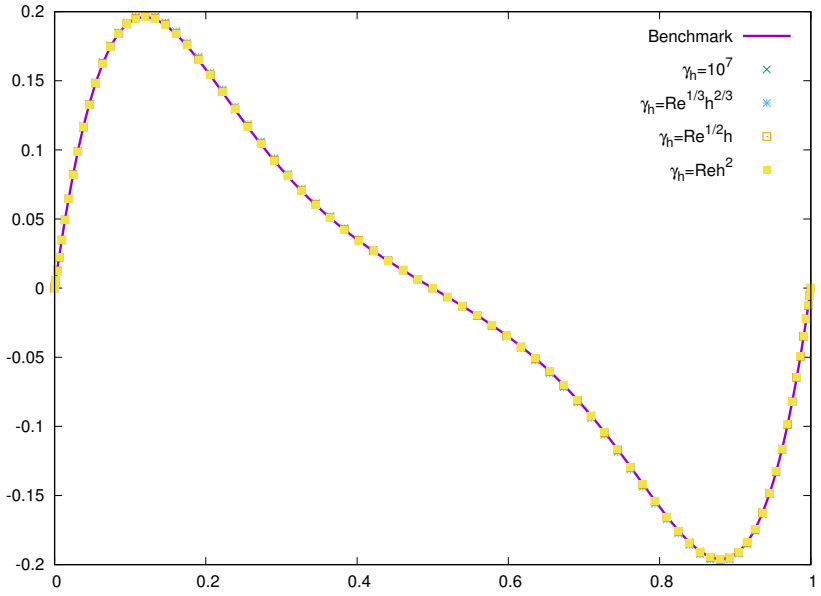

Figure 1: Case NC−Sq: vertical velocity profile at $y = 0.5$; comparison with results from [30]. The mesh size is $h = 1/80$.

	$\gamma_h \sim 10^{-7}$		$\gamma_h \sim Re^{1/3}h^{2/3}$		$\gamma_h \sim Re^{1/2}h$		$\gamma_h \sim Re\,h^2$	
h	err	rate	err	rate	err	rate	err	rate
1/20	2.34E-02		7.73E-03		1.15E-02		1.46E-02	
1/40	2.17E-02	0.11	4.05E-03	0.93	7.22E-03	0.67	1.36E-02	0.10
1/80	2.10E-02	0.04	2.13E-03	0.93	4.32E-03	0.74	1.33E-02	0.04
1/160	2.08E-02	0.02	1.15E-03	0.89	2.51E-03	0.78	1.31E-02	0.01
1/320	2.07E-02	0.01	7.13E-04	0.69	1.46E-03	0.79	1.31E-02	0.01

Table 18: Case NC−Sq : $\|\boldsymbol{p} - \boldsymbol{p}_h\|_{L^2}$ for P_1-P_1-P_1 elements

Once again, the results are in accordance with the theoretical results, even though the case $\gamma_h = Re\ h^2$ exhibits slightly better results than expected.

We strengthen our code validation by comparing the final state with a profile obtained by a spectral code [30]. The vertical v_{FE} velocity profile is extracted at mid-domain ($y = 0.5$) and plotted in Figure 1 for the pair (P_1-P_1) and the different values of γ_h and compared to the reference solution v_{LQ}. The difference $\|v_{FE} - v_{LQ}\|_{L^2}$ is reported in Table 19.

	$\gamma_h = 10^{-7}$		$\gamma_h = Re^{1/3}h^{2/3}$		$\gamma_h = Re^{1/2}h$		$\gamma_h = Re\,h^2$	
h	err	rate	err	rate	err	rate	err	rate
1/20	5.08E-03		7.76E-03		5.14E-03		4.85E-03	
1/40	6.01E-04	3.08	1.55E-03	2.32	6.32E-04	3.02	5.57E-04	3.12
1/80	7.09E-05	3.08	4.29E-04	1.85	8.30E-05	2.93	6.43E-05	3.11
1/160	7.36E-06	3.27	1.42E-04	1.60	1.09E-05	2.93	6.59E-06	3.29
1/320	7.34E-07	3.33	1.01E-05	3.82	1.24E-06	3.13	6.29E-07	3.39

Table 19: Case NC−Sq: error on the centerline velocity $\|v_{FE} - v_{LQ}\|_{L^2}$.

Differences decrease when the mesh resolution is increased. Our comparison with the spectral code guarantees that our code gives a correct final solution. The numerical results for these different cases demonstrate the validity of Corollary (44). The numerical results we presented confirm that the choice of $\gamma_h = Re^{1/3}h^{2/3}$ is suitable to obtain convergence on both velocity and pressure, but with non optimal rate $2/3$ for the velocity. If one is interested only in the velocity accuracy, then the choice $\gamma_h = Re^{1/2}h$ yields the best convergence rate on the velocity, while loosing convergence on the pressure. In summary, these two choices along with P_1-P_1 finite elements are suitable for simulating natural convection problems.

6.2.3 Rayleigh-Bénard natural convection in a square (case NC−RB)

We finally illustrate the good behaviour of the low order finite element on the classical Rayleigh-Bénard benchmark. In this setting, we consider a square cavity, with imposed temperature at the top (cold temperature) and the bottom (hot temperature). We compute a steady state for different values of the Rayleigh number, and compute the (averaged) Nusselt number at the hot wall as

$$\mathcal{N}u = \int_0^1 (-\partial_y \theta)_{|y=0}\ dx.$$

We compare our results to the ones reported in [31] (finite volume method) and [32] (Taylor-Hood finite element method with prediction scheme) and report the results in Table 20.

Ra	$\gamma_h = Re^{1/2}h$	$\gamma_h = Re^{1/3}h^{2/3}$	ref. [31]	ref. [32]
10^4	2.1591	2.1615	2.1581	2.1585
10^5	3.9167	3.9252	3.9103	3.9150
10^6	6.3059	6.2894	6.3092	6.3094

Table 20: Case NC−RB: average Nusselt number at the hot wall for different values of Ra. (P_1-P_1-P_1) computations with mesh resolution $h = 1/256$ (same as the reference computations).

Despite the low order (P_1-P_1-P_1), our results are in good agreement with published results obtained with the same mesh resolution. The largest difference is observed for $Ra = 10^5$ and is less than 0.4%.

6.3 Computational cost

6.3.1 2D-Natural Convection

As stated before, the non linear system (29)-(30)-(31) is solved using a Newton algorithm. The number of Newton iterations does not change when changing the order of the polynomials. Thus, using a direct solver for the linear systems that are involved ensures a computational gain for the linear element compared to the quadratic element.

However, it is worth mentioning that, the use of an iterative solver (e.g. GMRES as in our simulations) yields a reduction of the computational cost, even though the resulting systems are more ill-conditioned.

We compare the computation time between (P_1-P_1-P_1) and (P_2-P_1-P_2) finite elements for some of the previously tested cases. In parallel, we compare the number of degrees of freedom for both pairs related to the mesh size h. Since we observe similar behaviours for different values of h, we report in Table 21 the values for $h = 1/160$. The number of degrees of freedom for the (P_2-P_1-P_2) is about three times that of (P_1-P_1-P_1) elements.

	Case `NC-Nour`			Case `NC-Sq`		
γ_h	P_1-P_1-P_1	P_2-P_1-P_2	ratio	P_1-P_1-P_1	P_2-P_1-P_2	ratio
10^{-7}	40 683	8 641	0.21	84 282	16 607	0.20
$Re^{1/3}h^{2/3}$	2 465	8 371	3.40	3 432	12 438	3.62
$Re^{1/2}h$	2 419	8 424	3.48	4 499	12 714	2.83
$Re\,h^2$	2 470	8 575	3.47	13 951	14 591	1.05
ndof	103 684	335 044	3.23	103 684	335 044	3.23

Table 21: CPU-time (s) for different choices of γ_h, with $h = 1/160$. The "ratio" columns contains the ratio between the CPU-time for the P_2-P_1-P_2 computation and the CPU-time for the P_1-P_1-P_1 computation.

It is interesting to note that the choice of γ_h with Taylor-Hood elements (P_2-P_1) for velocity and pressure, and P_2 for temperature does not affect the computational time, while it has a visible impact for the (P_1-P_1-P_1) computations. The choices $\gamma_h \sim Re^{1/3}h^{2/3}$ and $\gamma_h \sim Re^{1/2}h$, for which we have proven convergence of the scheme, give the smallest computation times. This choices also bring a noticeable gain compared to P_2 computations.

We conclude this section by assessing the choice of γ_h when used with Taylor-Hood finite elements. In particular, the choice $\gamma_h \simeq h$ reduces the expected order of convergence. For a better choice of γ_h, error estimates might be established at the cost of extra regularity of the solution, or without using the modified projection. In the latter case, the order of convergence will be limited by γ_h. In Figure 2, we report the computed errors on the velocity for the case `NC-Nour` with respect to the CPU time needed for the computations.

It can be seen that the use of low order finite elements is equivalent to the Taylor Hood element with the same stabilization term. For the sake of completeness, we also provide results for Taylor-Hood computations without stabilization, which exhibits (as expected) a better behaviour owing to the higher order of accuracy. This is also due to the second order in time discretization used in our toolbox. With only first order scheme, the order of convergence for Taylor-Hood elements would be affected, thus reducing the overall accuracy.

6.3.2 3D Natural Convection

We now consider the same case of natural convection of air described in 6.1.2 and add the third dimension in space. We thus simulate the thermally driven cubic cavity $[0, 1]^3$, filled with air. The temperature is fixed on the left (hot) wall surface and the right (cold) wall surface. All the other lateral surfaces are adiabatic. No-slip walls are applied for the velocity on all boundary surfaces. Simulations are made for $Ra = 10^4$ on a fixed and uniform mesh with $h = 1/40$ for the finite element pairs (P_1-P_1-P_1) and (P_2-P_1-P_2). CPU-time for different values of γ_h is given in Table 22.

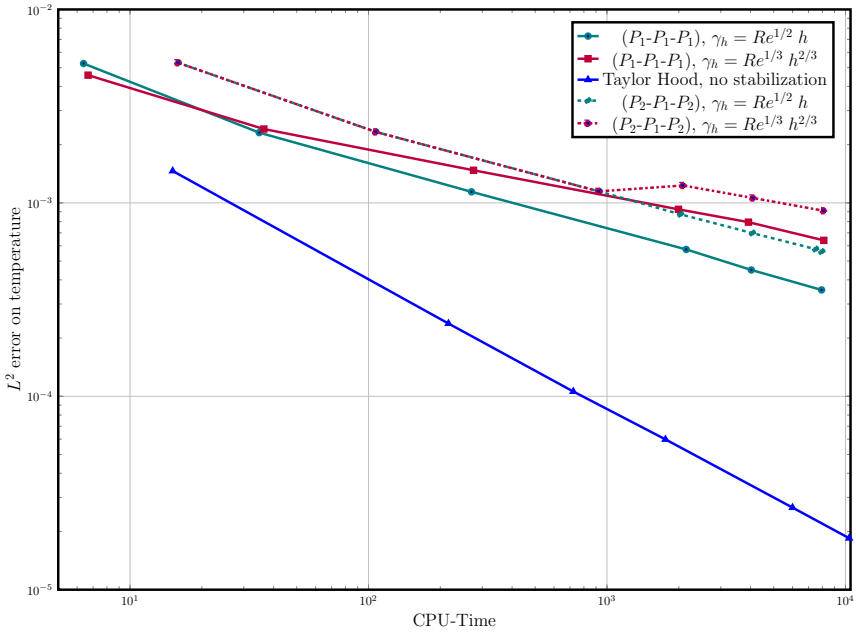

Figure 2: Case `NC-Nour`*: L^2 error on the temperature with respect to CPU time.*

γ_h	P_1-P_1-P_1	P_2-P_1-P_2	ratio
10^{-7}	7 761	20 059	2.62
$Re^{1/3}h^{2/3}$	5 476	17 699	3.23
$Re^{1/2}h$	5 713	17 964	3.14
$Re\, h^2$	6 043	19 084	3.16
ndof	344 605	2 194 685	6.37

Table 22: CPU-time for 3D-Natural-Convection.

As for the 2D case, we observe a non negligible reduction in the computational time, which supports the use of low-order finite elements.

7 Conclusion

We introduced a new projection operator to establish an error estimate for the approximation of the natural convection problem with linear elements. Using this operator and choosing a stabilization γ_h accordingly, we are able to recover almost first order accuracy in space. The error estimates on the projection and for the natural convection problem are validated with extensive examples, which indicate that the predicted convergence rate is optimal. Moreover, the choice of the stabilization parameter can be done in two ways. Using $\gamma_h \sim Re^{1/2}h$ gives a better convergence for the velocity, but does not yield any convergence for the pressure. Using $\gamma_h \sim Re^{1/3}h^{2/3}$ would allow a slow convergence in pressure, even though it reduces the accuracy for the velocity. In both cases, the computational time is reduced, when compared to the standard Taylor-Hood elements for the fluid equations. This makes the suggested scheme tractable for applications, even for 3D problems.

Preliminary simulations (not shown here) suggest that low order finite element approximation might also be used for more complex applications, such as simulation of PCM (e.g. cases presented in [1, 4]). This remains to be proven

using similar techniques : however, the analysis of convergence is more involved, due to the phase change which adds non linear terms in the energy equation.

References

[1] A. Rakotondrandisa, G. Sadaka, I. Danaila, A finite-element toolbox for the simulation of solid-liquid phase-change systems with natural convection, Computer Physics Communications 253 (2020) 107188.

[2] A. G. Zimmerman, J. Kowalski, Mixed finite elements for convection-coupled phase-change in enthalpy form: open software verified and applied to 2D benchmarks, Computers & Mathematics with Applications 84 (2021) 77–96.

[3] M. El-Hadda, Y. Belhamadia, J. Deteix, D. Yakoubi, A projection scheme for phase change problems with convection, Computers & Mathematics with Applications (2022) 109–122.

[4] G. Sadaka, A. Rakotondrandisa, P.-H. Tournier, F. Luddens, C. Lothodé, I. Danaila, Parallel finite-element codes for the simulation of two-dimensional and three-dimensional solid-liquid phase-change systems with natural convection, Computer Physics Communications 257 (2020) 107492.

[5] Y. Belhamadia, A. Kane, A. Fortin, An enhanced mathematical model for phase change problems with natural convection, International Journal of Numerical Analysis and Modeling, Series B 2 (2012).

[6] Y. Belhamadia, A. Fortin, T. Briffard, A two-dimensional adaptive remeshing method for solving melting and solidification problems with convection, Numerical Heat Transfer, Part A: Applications 76 (2019) 1–19.

[7] R. Aldbaissy, F. Hecht, G. Mansour, T. Sayah, A full discretisation of the time-dependent Boussinesq (buoyancy) model with nonlinear viscosity, Calcolo 55 (4) (2018) 49, id/No 44.

[8] A. Ern, J.-L. Guermond, Finite elements: Theory, applications, implementation, Vol. 36, Berlin: Springer, 2002.

[9] T. Chacón Rebollo, M. Gómez Mármol, V. Girault, I. Sánchez Muñoz, A high order term-by-term stabilization solver for incompressible flow problems, IMA J. Numer. Anal. 33 (3) (2013) 974–1007.

[10] J. de Frutos, B. García-Archilla, V. John, J. Novo, Error analysis of non inf-sup stable discretizations of the time-dependent Navier-Stokes equations with local projection stabilization, IMA J. Numer. Anal. 39 (4) (2019) 1747–1786.

[11] J. Li, Y. He, A stabilized finite element method based on two local Gauss integrations for the Stokes equations, J. Comput. Appl. Math. 214 (1) (2008) 58–65.

[12] Y. Zhang, Y. Hou, J. Zhao, Error analysis of a fully discrete finite element variational multiscale method for the natural convection problem, Comput. Math. Appl. 68 (4) (2014) 543–567.

[13] E. Burman, M. A. Fernández, Galerkin finite element methods with symmetric pressure stabilization for the transient Stokes equations: stability and convergence analysis, SIAM J. Numer. Anal. 47 (1) (2009) 409–439.

[14] F. Brezzi, M. Fortin, Mixed and hybrid finite element methods, Vol. 15, New York etc.: Springer-Verlag, 1991.

[15] T. Kashiwabara, I. Oikawa, G. Zhou, Penalty method with P1/P1 finite element approximation for the Stokes equations under the slip boundary condition, Numer. Math. 134 (4) (2016) 705–740.

[16] D. Adak, S. Natarajan, On the H^1 conforming virtual element method for time dependent Stokes equation, Mathematics in Computer Science.

[17] J. Shen, Pseudo-compressibility methods for the unsteady incompressible Navier-Stokes equations.

[18] J. Boland, W. Layton, An analysis of the finite element method for natural convection problems, Numer. Methods Partial Differ. Equations 6 (2) (1990) 115–126. doi:10.1002/num.1690060202.

[19] H. W. J. Lenferink, An accurate solution procedure for fluid flow with natural convection, Numer. Funct. Anal. Optim. 15 (5-6) (1994) 661–687. doi:10.1080/01630569408816586.

[20] J. Woodfield, M. Alvarez, B. Gómez-Vargas, R. Ruiz-Baier, Stability and finite element approximation of phase change models for natural convection in porous media, J. Comput. Appl. Math. 360 (2019) 117–137.

[21] R. Oyarzúa, P. Zúñiga, Analysis of a conforming finite element method for the Boussinesq problem with temperature-dependent parameters, J. Comput. Appl. Math. 323 (2017) 71–94.

[22] E. Di Nezza, G. Palatucci, E. Valdinoci, Hitchhiker's guide to the fractional Sobolev spaces, Bulletin des Sciences Mathématiques 136 (2012) 521–573.

[23] F. Brezzi, On the existence, uniqueness and approximation of saddle-point problems arising from Lagrangian multipliers, Revue française dautomatique, informatique, recherche opérationnelle. Analyse numérique 8 (R2) (1974) 129–151.

[24] V. Girault, P.-A. Raviart, Finite Element Methods for Navier-Stokes Equations: Theory and Algorithms, Vol. 5 of Springer Series in Computational Mathematics, Springer Berlin / Heidelberg, Berlin, Heidelberg, 1986.

[25] P. Ciarlet Jr, Analysis of the Scott-Zhang interpolation in the fractional order Sobolev spaces, J. Numer. Math. 21 (3) (2013) 173–180.

[26] H. Beirão da Veiga, A new approach to the L^2-regularity theorems for linear stationary nonhomogeneous Stokes systems, Portugaliae Mathematica 54.

[27] F. Hecht, New developments in FreeFem++, Journal of Numerical Mathematics 20 (2012) 251–266.

[28] F. Hecht, O. Pironneau, A. L. Hyaric, K. Ohtsuka, FreeFem++ (manual), www.freefem.org, 2007.

[29] R. Nourgaliev, H. Luo, B. Weston, A. Anderson, S. Schofield, T. Dunn, J.-P. Delplanque, Fully-implicit orthogonal reconstructed discontinuous Galerkin method for fluid dynamics with phase change, Journal of Computational Physics 305 (2016) 964–996.

[30] P. Le Quéré, Accurate solutions to the square thermally driven cavity at high Rayleigh number, Computational Fluids 20 (1991) 24–41.

[31] N. Ouertatani, N. Ben Cheikh, B. Ben Beya, T. Lili, Numerical simulation of two-dimensional Rayleigh-Bénard convection in an enclosure, Comptes Rendus Mécanique 336 (2008) 464–470.

[32] J. Deteix, A. Jendoubi, D. Yakoubi, A Coupled prediction scheme for solving the Navier-Stokes and convection-diffusion equations, SIAM J. Numer. Anal.